Catalyst Activation by Loss of Cyclopentadienyl Ligands in Hydrogen Transfer Catalysis with Cp^*Ir^{III} Complexes

Jesús Campos,[†] Ulrich Hintermair,[†§] Timothy P. Brewster,[†#] Michael K. Takase,[†‡] and Robert H. Crabtree[†]**

[†] Department of Chemistry, Yale University, 225 Prospect Street, New Haven, Connecticut 06520, USA.

[§] Centre for Sustainable Chemical Technologies, University of Bath, Claverton Down, Bath BA2 7AY, UK.

[#] Present address: Department of Chemistry, University of Washington, Seattle, Washington 98195, USA.

[‡] Present address: Division of Chemistry and Chemical Engineering, California Institute of Technology, Pasadena, California 91125, USA.

[§]u.hintermair@bath.ac.uk, [†]robert.crabtree@yale.edu

KEYWORDS

Transfer-hydrogenation, Cp*Ir complexes, Cyclopentadienyl ligands, N-heterocyclic carbenes, homogeneous catalysis.

ABSTRACT

The activity of the two related complexes $[Cp^*Ir(IMe)_2X]BF_4$ (X = Cl (**1**), H (**2**)) in transfer-hydrogenation from *iso*-propanol to acetophenone was investigated. These studies suggest that the commonly accepted monohydride mechanism for transfer-hydrogenation mediated by cyclopentadienyl iridium species does not apply to chloride **1**. We have found evidence that while the two monodentate NHC ligands are retained in the coordination sphere, the Cp* fragment is completely released under mild conditions in a precatalytic activation step. Synthesis of modified versions of the initial precatalyst **1** with different cyclopentadienyl and NHC ligands demonstrated that increasing the steric pressure around the iridium center facilitates precatalyst activation and thus enhances the catalytic performance. Study of five new iridium(III) complexes bearing mono or diphosphines helped us monitor Cp* ligand loss under mild conditions. An unusual P-C bond cleavage was also noted in a 1,2-bis(dimethylphosphino)methane (dmpm) ligand. Based on these findings, a novel catalyst activation mechanism is proposed for $[(\eta^5\text{-}C_5R_5)Ir]$ transfer-hydrogenation based on the lability of the cyclopentadienyl ligand.

INTRODUCTION

Catalytic hydrogen transfer reactions provide an attractive alternative to direct hydrogenation of a broad variety of substrates avoiding the need for molecular hydrogen.[1] Furthermore, the reversible nature of the ionic H^+/H^- transfer[2] has been exploited in 'borrowing-hydrogen' processes[3-6] for the formation of C-C, C-N and C-O bonds and also for the racemization of alcohols. Although transfer-hydrogenation reactions have been known for more than a century,[7] the first homogeneous catalytic systems did not appear until the late 1960s and were based on iridium compounds,[8-10] still one of the most widely used metals today.[11] The introduction of the versatile Cp*Ir catalyst precursors for these transformations was independently reported in the 2000s by Ikariya and Noyori[12,13] and Fujita and Yamaguchi.[14] Since then, there has been a dramatic increase in the number of Cp*Ir systems active for a wide variety of transfer-hydrogenation reactions,[15] and more recently the list has been enlarged to include very effective species containing N-heterocyclic carbene (NHC) ligands.[16,17] Several Cp*Ir precatalysts are currently commercially available, and the first industrial applications have been reported.[18]

Despite the importance of Cp*Ir compounds as precatalysts for transfer-hydrogenation reactions, we still have little insight into the effects of ligand substitution at the Cp*Ir fragment. In a previous contribution we studied a small library of Cp*Ir catalysts in hydrogen-transfer from alcohols to ketones,[19] comparing a number of spectator ligands under various reaction conditions. A novel Cp*Ir complex containing two minimally substituted, monodentate NHC ligands (**1** in Fig. 1) emerged as the most active precatalyst in the presence of KOH. We were able to rule out contributions from heterogeneous iridium metal, to show that both of the IMe (1,3-dimethyl-imidazol-2-ylidene) ligands were needed for efficient turnover, and to investigate the kinetics of the reaction. Additionally, a stable monohydride derivative (**2**), often considered a key

intermediate in these reactions, could be isolated and found to be an active precatalyst for transfer-hydrogenation of acetophenone from excess *iso*-propanol in the presence of KOH.

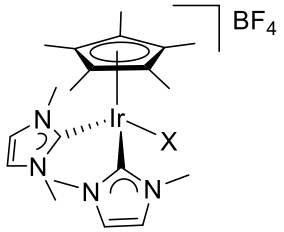

X = Cl (**1**); H (**2**)

Figure 1. Cp*Ir precatalysts for transfer hydrogenation from alcohols to ketones.[19]

Two mechanisms are commonly proposed for metal-catalyzed transfer-hydrogenation reactions:[20] i) the hydridic route and ii) direct hydrogen transfer. In the former case a metal hydride is involved in the hydrogen transfer step, whereas in the latter the metal facilitates direct hydride transfer between substrate and product by providing a six-membered cyclic transition state (**A** in Fig. 2). The direct pathway was initially proposed for the Meerwein-Ponndorf-Verley (MPV) reduction,[9,21] although recent computational work also supported its relevance to some iridium-based systems.[22] Nevertheless, hydridic mechanisms are most commonly proposed for transition metal catalyzed reactions. These have been further divided into monohydride or dihydride classes, where the former has been shown to operate both by inner-sphere (**B**)[20] and, less frequently, outer-sphere (**C**) pathways.[23]

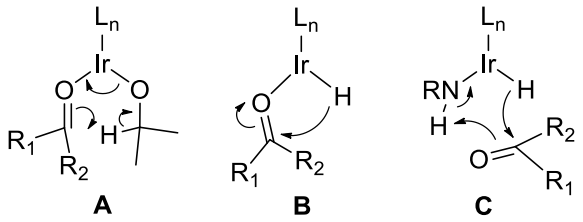

Figure 2. Key intermediates in common transfer hydrogenation reaction mechanisms: direct hydrogen transfer (**A**); inner-sphere monohydride route (**B**); outer-sphere monohydride route (**C**). L_n denotes non-functional spectator ligands.

The commonly accepted mechanism for Cp*Ir-catalyzed hydrogen transfer reactions is the monohydride route (either inner or outer-sphere),[24,22,25] that assumes full retention of all ancillary ligands,[20] although the dihydride pathway has less frequently been proposed.[17] In our previous work, the kinetics of the reaction with **1** were found to be unexpectedly complex and H/D scrambling experiments, often used to probe the mechanism of these reactions,[26] gave inconclusive results. We thus felt that the mechanism of hydrogen transfer catalysis with these complexes required a closer look in order to unravel the role of monohydride **2** in catalysis. Here we provide new experimental data that rule out the classic routes for our Cp*Ir^{III} systems and suggest a new alternative pathway for this type of catalyst.

RESULTS AND DISCUSSION

In the full cycle of the classical base-assisted monohydride pathway of Scheme 1,[26] the hydride is delivered by the metal and the proton shuttled by an external base. Under reaction conditions, the chloride precursor **1** is converted into the alkoxide complex **D**, which undergoes β-H elimination (BHE) to generate the monohydride species **2**. Hydride delivery (HDE) from **2** would

then provide alkoxide complex **D'**, and after product dissociation either precatalyst **1** or alkoxide species **D** is regenerated. An important aspect of this mechanism is that the two main steps, namely BHE and HDE, generally require the presence of two adjacent vacant sites on the iridium.[27] However, both alkoxide **D** and hydride **2** are coordinatively and electronically saturated, and we have previously shown that both IMe ligands are needed for good catalytic performance and thus likely retained throughout the cycle. Outer-sphere Noyori-type monohydride pathways circumvent substrate coordination to the metal through concerted LH^+/MH^- transfer and thus proceed with one open site on the metal (**C** in Fig. 2),[23] however this metal-ligand cooperation seems rather unlikely with the ligand framework of **1**. Cp* has been suggested to be able to act as a transient inner-sphere base[28] to facilitate formation of the required $Ir^{III}H$ in a Noyori-type mechanism based on DFT calculations, but experimental evidence for such a mechanism has not been found yet. In related coordinatively saturated $[(arene)RuL_n]^+$ catalysts, η^6-η^4 ring slippage of the arene has been proposed to allow for the formation the corresponding monohydride from alkoxide intermediates.[29] In another related case, a Ru-OMe unit is converted into its Ru-H analog presumably *via* ring slippage.[30]

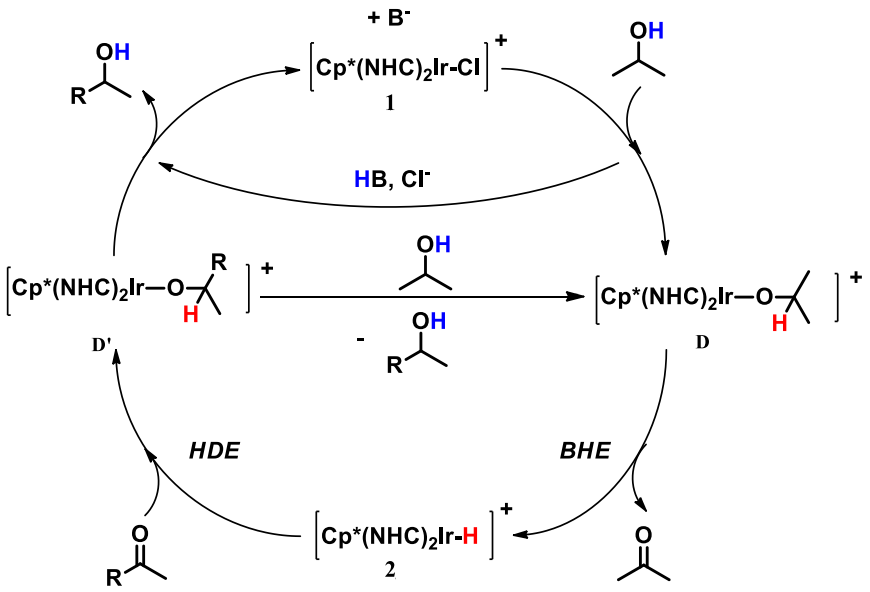

Scheme 1. Inner-sphere monohydride mechanism of base-assisted hydrogen transfer from alcohols to ketones mediated by Cp*Ir(NHC)$_2$ complexes (B = base).

Mechanistic Studies

In all scenarios following the mechanism shown in Scheme 1, both hydride **2** and halide **1** would be in-cycle intermediates, and as such should provide similar performance in catalysis. However, while **2** provided some activity in transfer hydrogenation catalysis, it was clearly less efficient than **1** and gave a different degree of H/D scrambling in the reduction of acetophenone by *iso*-propanol.[19] Comparing reaction profiles at 60 ºC further corroborated the considerably lower activity of monohydride **2** with respect to chloride **1** (Figure 3). Similar observations made previously for [(arene)Ru] transfer-hydrogenation catalysts have led to the conclusion that the less active monohydride was not a catalytic intermediate.[31,32] Additional interesting results emerged from these data: i) whereas **1** required a base to be active in catalysis, the efficiency of the related hydride was unchanged in its absence; (ii) while transfer-hydrogenation catalyzed by **1** exhibits a characteristic induction period of several minutes, as previously reported,[19] compound **2** was immediately active. This result suggests that a preactivation step is required only for catalysis with **1**, while monohydride **2** is either an active species itself or gives easier access to an active catalyst; iii) Using a 1:1 mixture of **1** and **2** did not improve the catalytic performance, instead the overall rate was just the sum of the independent profiles for **1** and **2**. This finding disfavors a bimolecular mechanism involving hydride **2**, suggesting that each complex may operate in distinct cycles.

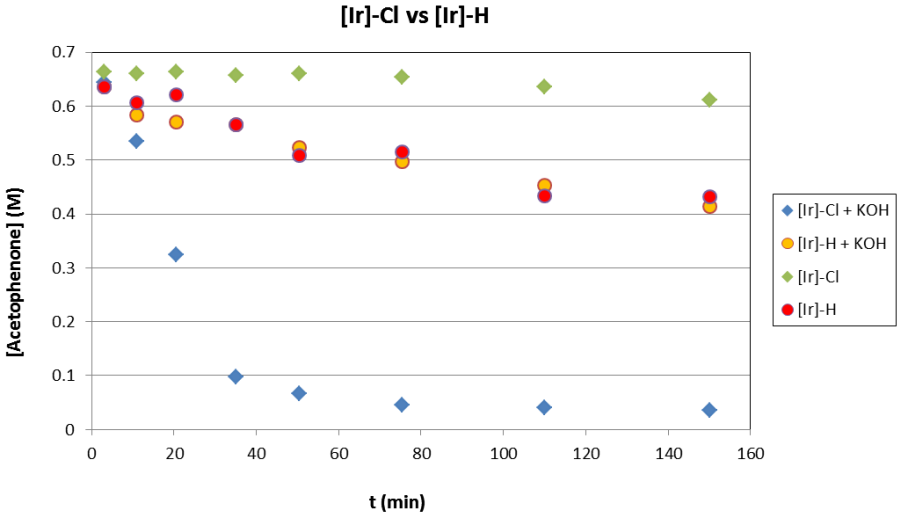

Figure 3. Reaction profiles of transfer hydrogenation of acetophenone from excess *iso*-propanol with **1** and **2** in the presence and absence of base at 60 ºC. Reaction conditions: 2 mmol substrate, 1 mol% [Ir], 3 mL ^{i}PrOH, 60 ºC, N_2 (^{1}H NMR analysis with 1,3,5-trimethoxybenzene as internal standard).

We previously synthesized monohydride **2** by the reaction of **1** with $NaBH_4$, but we have now attempted to prepare **2** from alkoxides relevant to catalysis to investigate the viability of β-H elimination (see Scheme 1). When heating a solution of **1** in ^{i}PrOH with excess potassium hydroxide the reaction mixture quickly turned dark red, as also seen in the early stages of catalysis with **1** in the presence of substrate. However, we were unable to isolate or characterize alkoxide derivatives of **1** either with *iso*-propanol or methanol. Even with alcohols lacking β-hydrogens such as *tert*-butanol or catechol at low temperature and under inert atmosphere, the expected alkoxides could not be observed by ^{1}H NMR. We did, however, detect a number of distinctive high-field ^{1}H NMR signals characteristic of metal hydrides in the region from -15.5 to -16.5 ppm after heating **1** in the presence of excess Na^{i}OPr (Figure 4). The number and distribution of ^{1}H

NMR peaks in this region was dependent on the solvent employed. Among the hydride species observed, compound **2** was present as a minor reaction product (*ca*. 20 %) when the reaction was carried out in CD_2Cl_2 (Figure 4B). When the same reaction was performed in *iso*-propanol (Figure 4D), the hydridic region of the ^1H NMR spectrum displayed peaks related to those observed after a transfer-hydrogenation catalytic run using **1** (Figure 4E). This suggests that the catalytically active species is related to one (or several) of these iridium hydrides. In contrast, the related hydride **2** remained essentially unaltered under similar catalytic conditions even after full conversion of 100 equivalents of acetophenone to 1-phenylethanol (Figure 4F and 4G). We cannot exclude compound **2** being one of the competent intermediates in catalysis by **1**, but one or several of the other iridium-hydrides generated under the reaction conditions likely exhibits considerably enhanced catalytic activity thereby dominating the catalytic performance of the much more active precatalyst **1**. Moreover, the fact that we do observe reduction of acetophenone mediated by the hydrido species **2**, albeit in lower yield, indicates either a dissimilar mechanism operating for hydride **2** *versus* chloride **1**, or partial decomposition of the former to generate very small amounts (below the NMR detection limit) of an alternative active species.

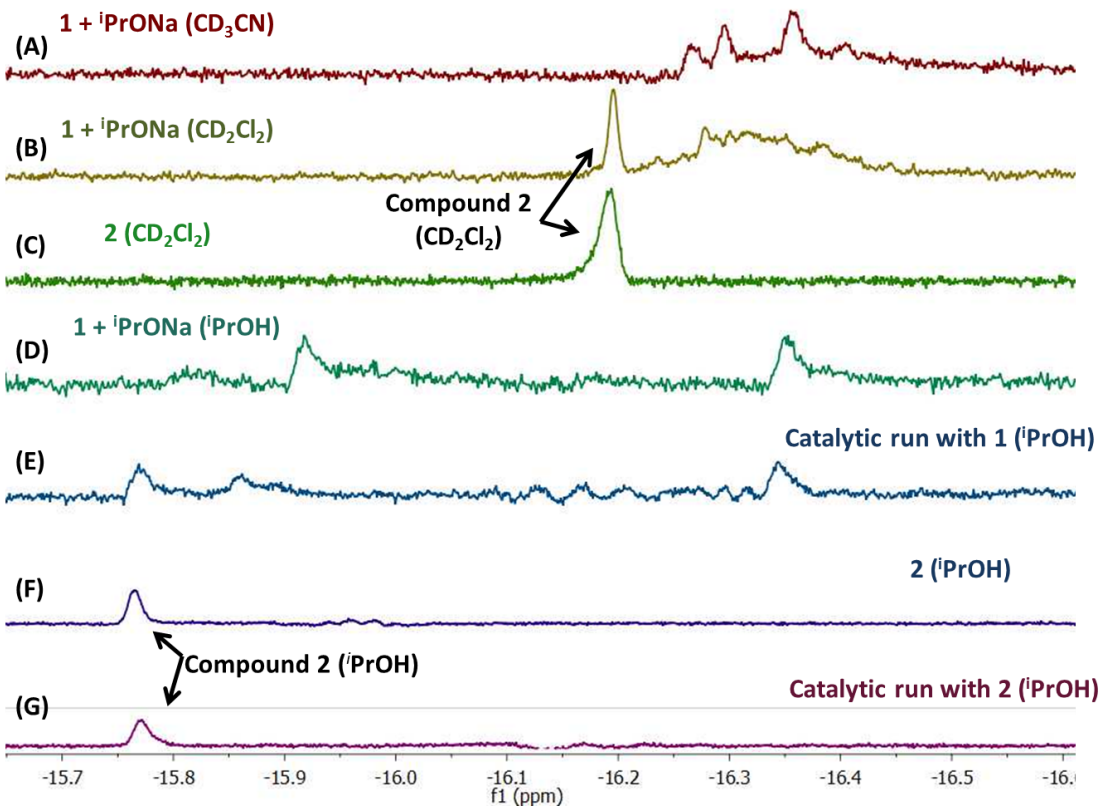

Figure 4. ^{1}H NMR hydride region of *in-situ* reactions carried out in sealed NMR tubes using TMB as internal standard. (A) A solution of **1** and ^{i}PrONa (5 equiv) in CD_3CN heated at 60 ºC for 1 hour; (B) A solution of **1** and ^{i}PrONa (5 equiv) in CD_2Cl_2 heated at 45 ºC for 3 hours; (C) Compound **2** in CD_2Cl_2; (D) A solution of **1** and ^{i}PrONa (5 equiv) in ^{i}PrOH heated at 60 ºC for 1 hour; (E) Catalytic transfer-hydrogenation from ^{i}PrOH (1 mL) to acetophenone (78 µL) in the presence of **1** (1 mol %) and KOH (10 mol %) after 3 hours at 60 ºC (99 % ketone reduction); (F) Catalytic transfer-hydrogenation from ^{i}PrOH (1 mL) to acetophenone (78 µL) in the presence of **2** (1 mol %) and KOH (10 mol %) prior to heating (0 % ketone reduction). (G) Catalytic transfer-hydrogenation from ^{i}PrOH (1 mL) to acetophenone (78 µL) in the presence of **2** (1 mol %) and KOH (10 mol %) after 3 hours at 60 ºC (55 % ketone reduction).

In our prior report[19] we made use of the deuterium labeling strategy proposed by Bäckvall and co-workers to distinguish monohydride and dihydride mechanisms.[26] The results showed different degrees of deuterium incorporation at the carbonyl carbon in the product depending on the precatalyst used, **1** or **2**, suggesting different mechanisms for each. Here we extend the comparison by investigating the electronic influence of different substituents on the substrate, kinetic isotopic effects (KIEs), and selectivity towards reduction of C=O *versus* C=C bonds. Table S1 (see supporting information) summarizes our results for transfer-hydrogenation from *iso*-propanol to *para*-substituted acetophenones. Whereas chloro- and iodo-derivatives were completely reduced using **1**, 89 % conversion was measured for the methoxy-substituted ketone under the same conditions, suggesting that electron-donating substituents have a detrimental effect on catalytic performance. To analyze this trend in more detail we performed Hammett studies[33] under competitive and non-competitive conditions with a number of *para*-substituted acetophenones (Figure 5, Figure S1 and Table S2).[19] The positive slopes of the observed Hammett correlations under non-competitive conditions (1.68 and 1.91 for **1** and **2**, respectively) indicate that in both cases negative charge is built up in the transition state of the turnover limiting step (TLS), consistent with a hydride delivery pathway such as HDE in Figure 2 being the TLS. As expected, similar results were obtained under *in situ* competitive conditions (1.65 and 1.94 for **1** and **2**, respectively). Kinetic isotopic effects (KIEs) are also consistent with this hypothesis. Under non-competitive conditions the primary KIEs measured were 2.2 ± 0.2 and 2.1 ± 0.2 for **1** and **2**, respectively, and slightly lower but similar values (1.8 (**1**) and 1.9 (**2**) ± 0.2) were obtained under competitive conditions (see Experimental Part for details).

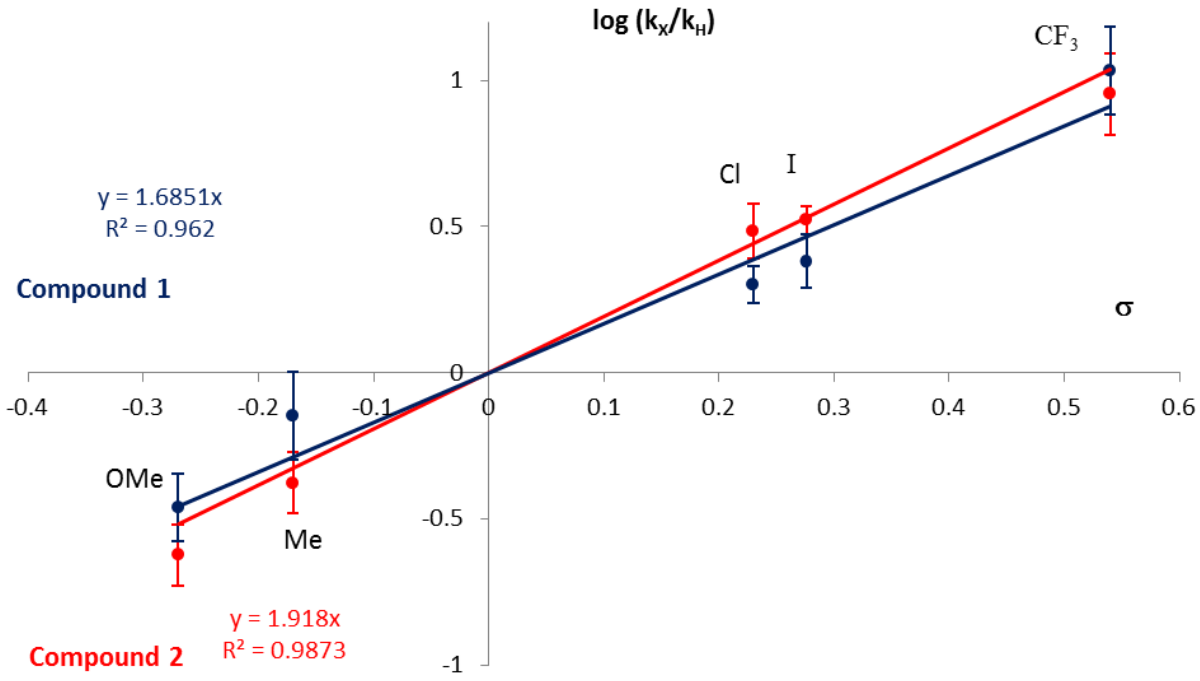

Figure 5. Hammett plots for catalysts **1** (blue) and **2** (red) obtained from non-competitive experiments for the transfer hydrogenation from isopropanol to *p*-substituted acetophenones (for details see the Supporting Information).

Next, the chemoselectivity of both catalysts towards reduction of C=O and C=C bonds was examined. In our previous report we observed that α,β-unsaturated ketones were completely reduced to their saturated alcohols using complex **1**.[19] Here we demonstrate that the reduction of C=C bonds is not restricted to conjugated substrates. Under our standard transfer-hydrogenation conditions (1 mol % [Ir], 10 mol % KOH, 60 ºC) styrene was converted into ethylbenzene in *ca.* 50 % yield after 5 hours using precatalyst **1**, whereas monohydride **2** showed no conversion under identical conditions (Scheme 2). Accordingly, complex **1** was able to reduce both C=O and C=C bonds of 5-hexen-2-one to yield 2-hexanol as the major product (*ca.* 85 %), along with minor amounts (*ca.* 8 %) of 5-hexen-2-ol and other unidentified species (Scheme 2). However, hydride **2** cleanly provided the olefinic alcohol as the main product in 95 % yield. While the selectivity

exhibited by **2** is in accordance with a classic catalyst proceeding through monohydride pathways, the ability of precatalyst **1** to reduce non-activated C=C bonds suggest the involvement of polyhydride species.[19]

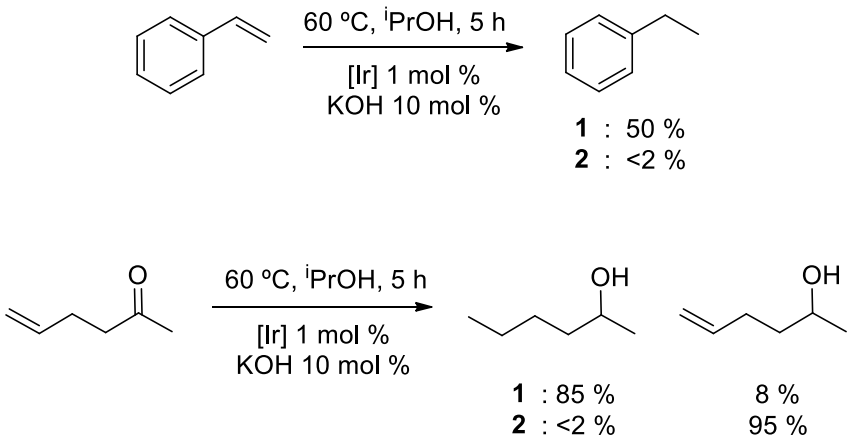

Scheme 2. Selective reduction of C-O *versus* C-C bonds

Comparing the lability of Cp* versus NHC

The collective evidence suggesting differential reactivity between **1** and **2** rules out a traditional monohydride mechanism for compound **1**, because **2** would be an intermediate in either cycle. Since the H/D scrambling results and C=C vs. C=O selectivity data suggested the involvement of multiple hydrides in the more efficient precatalyst **1**, we became dissatisfied with the standard monohydride mechanisms. Alternatively, formation of a dicationic Ir(V) dihydride intermediate might be proposed, but we believe that generation of such an species would not be favored under basic conditions due to the expected high acidity of the hydrides. Besides, it would not take into account the marked differences in reactivity between compounds **1** and **2**.

The loss of a C-donor ligand is not normally considered in mechanistic discussions of Cp*Ir-based catalysts, but some ligation rearrangement in **1** had to be operational to allow for the

formation of polyhydride species. To probe the relative lability of the NHCs versus the Cp* ligand, we introduced strongly binding phosphines to enhance steric stress around the metal to induce loss of the most easily dissociable ligand.[40,41] The reaction of compound **1** with excess PMe_3 and $Me_2PCH_2PMe_2$ (dmpm) at room temperature resulted in substitution of the chloride anion and formation of corresponding dicationic complexes **3** and **4**, which retain all the C-donor ligands (Scheme 3). Compound **3** is characterized by the appearance of a resonance in the $^{31}P\{^1H\}$ NMR spectrum at -46.9 ppm, whereas **4** displays two doublets at -38.7 and -53.1 ppm with a two-bond coupling constant of 34.9 Hz. In the ^1H NMR spectra a distinctive peak due to the Cp* ligand appears at 1.86 and 1.71 ppm for compounds **3** and **4**, respectively, exhibiting characteristic four-bond coupling to phosphorus of 2.3 Hz. The hindered rotation of the NHC ligands due to steric pressure brought by the phosphines is evidenced by the inequivalence of the backbone protons of the IMe ligands in the room temperature ^1H NMR spectra of **3** and **4** as opposed to the less congested complexes **1** or **2**. Compound **3** is stable to air in both the solid state and in solution. In contrast, exposure of solutions of **4** to air results in quantitative oxidation of the pendant phosphine ($t_{1/2} \approx 3$ hours with stirring) to yield complex **5**. A characteristic strongly deshielded $^{31}P\{^1H\}$ resonance at 41.4 (d, $^2J_{PP} = 29$ Hz) was recorded for **5**, confirming the formation of the phosphine oxide. The complete air-stability of **4** and the clean *mono*-oxidation of dmpm in **5** suggest that the phosphines remain tightly bound even in solution. Analysis of single crystals of **3** and **5** by X-ray diffraction (Figure 6) confirmed all structural features expected from the solution-phase NMR analysis. They display the standard piano-stool geometry and show typical Ir-P and Ir-C_{NHC} bond lengths, with values of 2.327(1) and 2.337(2)Å, for the Ir-P bonds of **3** and **5**, respectively, and 2.048(4), 2.089(4)Å and 2.031(7), 2.079(8)Å for the Ir-C_{NHC} bonds.

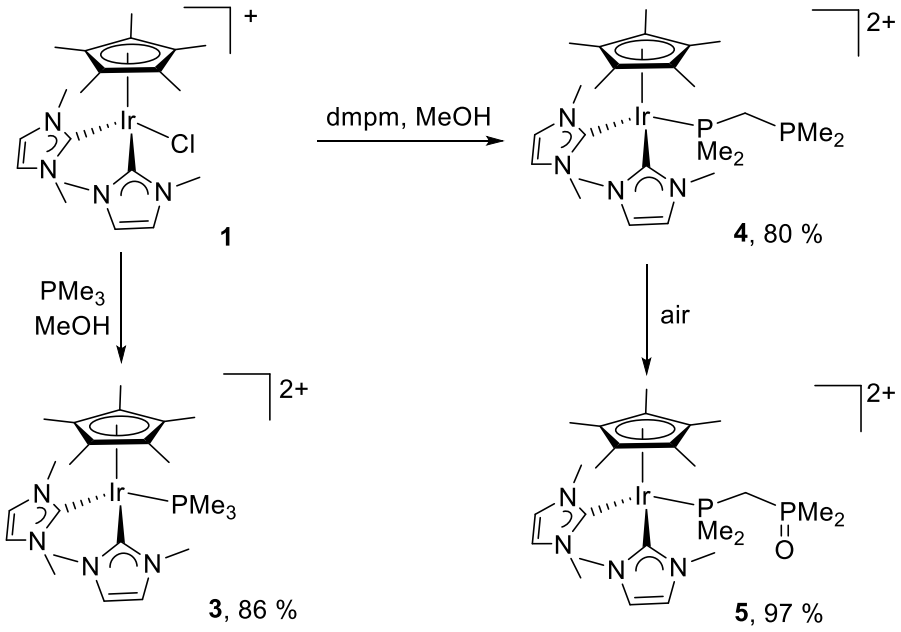

Scheme 3. Synthesis of dicationic phosphine derivatives of **1**.

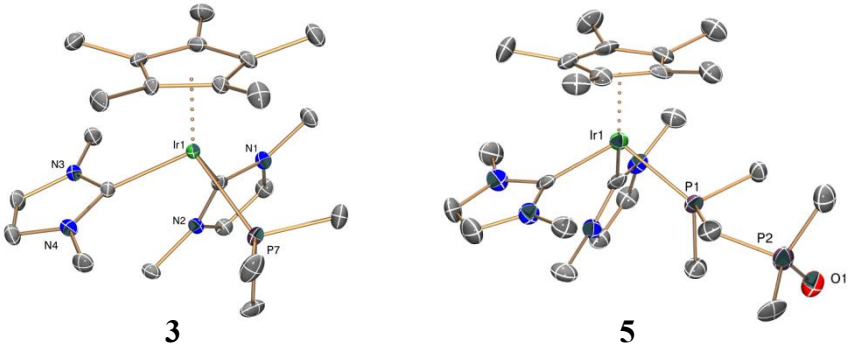

Figure 6. ORTEP diagrams of the cationic portions of compounds **3** and **5**. 50 % thermal ellipsoids are shown. Hydrogen atoms and solvent molecules have been omitted for clarity.

Heating methanol solutions of **3** under nitrogen at 60 ºC with excess PMe_3 (up to 50 equiv.) did not affect the integrity of the complex. Similarly, heating a solution of **4** at the same temperature did not result in any observable transformation or dynamic processes via ^{1}H or ^{31}P NMR spectroscopy. However, heating complex **4** with one additional equivalent of dmpm to 60 ºC

resulted in complete disappearance of ^{1}H and $^{31}P\{^{1}H\}$ NMR signals diagnostic of **4** within 10 min. The major product of the reaction (**6** in Scheme 4) resulted from dissociation of the Cp* ligand, while both NHCs remained bound to iridium. Compound **6** gives rise to four inequivalent signals in the $^{31}P\{^{1}H\}$ NMR spectrum (-43.1 (ddd, $^{2}J_{PP}$ = 63, 21, 18 Hz), -55.2 (ddd, $^{2}J_{PP}$ = 63, $^{4}J_{PP}$ = 21, 2 Hz,), -76.0 (ddd, $^{2}J_{PP}$ = 26, $^{4}J_{PP}$ = 21, 2 Hz), -93.4 ppm (m)), and a ^{1}H NMR high-field resonance at -14.8 ppm characteristic of an Ir–H with the expected coupling to the four phosphorus centers (ddt, 1 H, $^{2}J_{HP}$ = 150.0, 20.5, 5.3, $^{4}J_{HP}$ = 5.3 Hz). No peak arising from bound Cp* was present, whereas signals corresponding to the NHC fragments remained with only minor changes in the chemical shift from **4**. A minor species found in this reaction (**7** in Scheme 4) resulted from the substitution of the pendant CH_2PMe_2 fragment by an OMe group from the solvent, and was characterized by its three $^{31}P\{^{1}H\}$ resonances (54.4, -73.6 and -92.2 ppm) and a high field peak at -15.4 ppm in the ^{1}H NMR spectrum. Compound **6** could be isolated from the mixture as a pure white microcrystalline material by layering the methanol solution with diethyl ether. The structures of compounds **6** and **7** were further confirmed by X-ray diffraction, confirming complete displacement of the Cp* fragment (Figure 7). The hydride ligand appears bound to the iridium center *trans* to one of the phosphorus atoms of the chelated phosphine, whereas both NHCs are also *trans* to phosphorus. In both complexes, Ir-P and Ir-C_{NHC} distances have normal values.

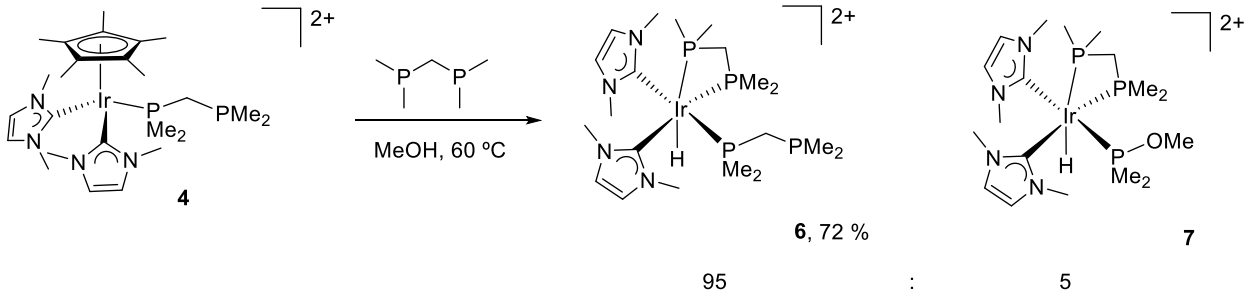

Scheme 4. Reaction of **4** with dmpm and subsequent Cp* displacement.

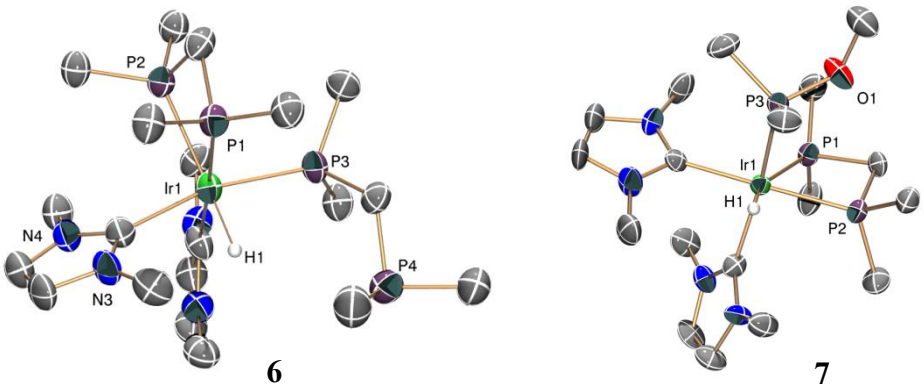

Figure 7. ORTEP diagrams of compounds **6** and **7**. 50 % thermal ellipsoids are shown. Hydrogen atoms (except Ir-H), counterions and solvent molecules have been omitted for clarity.

NHC dissociation by reductive elimination or ligand substitution is well documented,[34] a pathway that often has implications in catalysis.[35] However, our kinetic evidence that both IMe ligands are required for efficient catalysis (as reported in our prior paper[19]) along with the observed displacement of Cp* in compound **4** made us consider its possible loss under transfer-hydrogenation conditions. Cp* degradation in transition metal complexes has been reported under oxidative conditions,[36] but its dissociation is much less common in reducing or neutral environments. Main group complexes commonly display a variable hapticity of the Cp ligand[37,38] and frequently act as Cp transfer reagents.[39] Ring-slippage of η^5-C_5H_5 to η^3 and η^1-C_5H_5 is also well documented for a variety of transition metal complexes.[40] For instance, Casey found that in the presence of excess PMe_3, [η^5-(C_5H_5)Re(CH_3)(NO)(PMe_3)] is in equilibrium with related η^3- and η^1-C_5H_5 species, and the Cp is eventually released as $(C_5H_5)^-$ anion.[41] Although dissociation of Cp* is less frequent, it has been reported occasionally.[42] Cp* complexes of the rare earths are more ionic, and steric crowding can lead to dissociation of $(Me_5C_5)^-$.[43] We speculate that the formation of the iridium-hydride **6** might involve initial ring-slippage from η^5 to η^1-C_5Me_5 followed by β-H elimination to release a neutral fulvene species, although we cannot yet be sure.[44]

To the best of our knowledge this is the first example of dissociation of a Cp* ligand from an iridium complex to generate a single major product under mild conditions.

The fact that the Cp* ligand in compound **1** can be rapidly released using 2 equivalents of dmpm under mild heating may have direct implications in catalysis. The reaction of **1** and dmpm clearly indicates that the Cp* fragment in **1** is more labile than the NHC ligands, and that it prefers to dissociate completely rather than slip reversibly when sterically stressed. As discussed above, catalysis by **1** likely requires dissociation of one of the ligands that are usually considered spectators, Cp* or the NHCs, to produce the required vacant coordination sites. Although the reactivity displayed by **1** in the presence of phosphines or under ^{i}PrOH/KOH is not directly comparable, it is consistent with all our data to postulate that release of the Cp* rather than the NHC occurs during transfer-hydrogention. In fact, heating an *iso*-propanol solution of **1** in the presence of KOH (10 equiv) not only resulted in the appearance of several ^{1}H NMR resonances due to Ir-H units (*vide supra*), but also the rapid disappearance of the intense singlet at 1.65 ppm corresponding to bound Cp*. As before and in accord with related reports,[42a-c] all efforts to determine the chemical structure of the Cp* after release were unfruitful (including *in-situ* spiking of NMR samples with different Cp* derivatives, mass spectrometry and attempted separation by column chromatography for further spectroscopic analysis). Nevertheless, we were able to obtain useful indications from mass spectrometry analysis (FT-ICR) of a post-catalytic transfer-hydrogenation mixture. This showed a set of peaks consistent with the presence of $[Ir^{III}(IMe)_2(H)_2]^+$, a species in which Cp* loss has occurred (Figure S5; m/z = 385.1129 and 387.1151; calcd for $C_{10}H_{18}IrN_4^+$ = 385.1137 and 387.1161). Importantly, no Cp*Ir species was detected in this MS analysis. In our prior work[19] we described how molecular oxygen has a detrimental effect on the catalytic activity of **1**. Related to this, another set of peaks in the mass

spectrum indicates oxidation of the postulated dihydride species (Figure S5; m/z = 399.0922 and 401.0946; calcd. for $C_{10}H_{18}IrN_4O^+$ = 399.0930 and 401.0953). Taken together, these results strongly suggest that the active species in the case of the chloride complex **1** forms through dissociation of the Cp*.

Catalyst Preactivation

To test if the initial lag phase in catalysis with **1** was linked to Cp* loss as a pre-catalytic activation step, we set up parallel experiments in sealed NMR tubes. Reduction of acetophenone in ^{i}PrOH/KOH using 1 mol % of **1** was carried out at 25 ºC. In one case the NMR tube was heated at 60 ºC for 30 min prior to the addition of the ketone (Scheme 5). While 1-phenylethanol was formed in less than 2 % yield for the 25 ºC sample after 12 hours, 40 % conversion of acetophenone was seen from the thermally pre-activated catalyst. Analogous results were obtained when the catalytic reactions were monitored at 40 ºC. In this case, the 40 ºC sample gave 8 % conversion, while with the 60 ºC pre-activated sample the ketone was reduced in 70 % yield. Thus, the high temperatures required for transfer hydrogenation catalyzed by **1** are mainly needed for generating a more active iridium species through Cp* release.

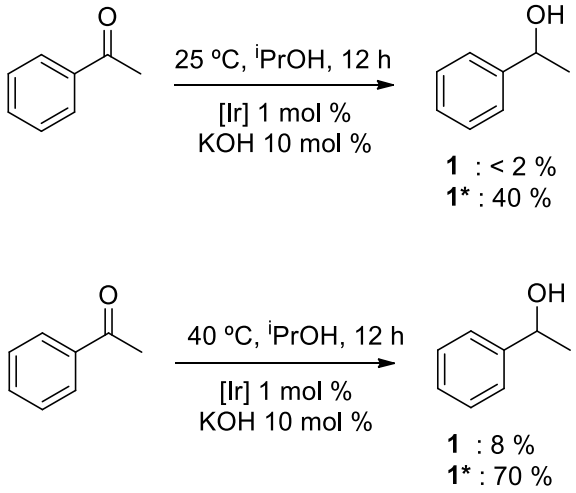

Scheme 5. Transfer-hydrogenation from ^{i}PrOH to acetophenone catalyzed by **1** and thermally pre-activated **1** (denoted **1***) (heating the reaction mixture at 60 ºC for 30 min prior to the addition of acetophenone).

New Catalyst Designs

To further test our hypothesis, we synthesized other derivatives with modified cyclopentadienyl and NHC ligands and tested them as precatalysts under our standard transfer-hydrogenation conditions. Compound **8**, first reported by Heinekey,[45] contains a chelating bis-NHC ligand. Compounds **9** and **10** bearing two NHC ligands were prepared *via* double carbene transfer from bis-NHC silver complexes to the corresponding cyclopentadienyl-iridium(III)-chloro dimers (Scheme 6, see Experimental Section for details), as previously reported.[46,19]

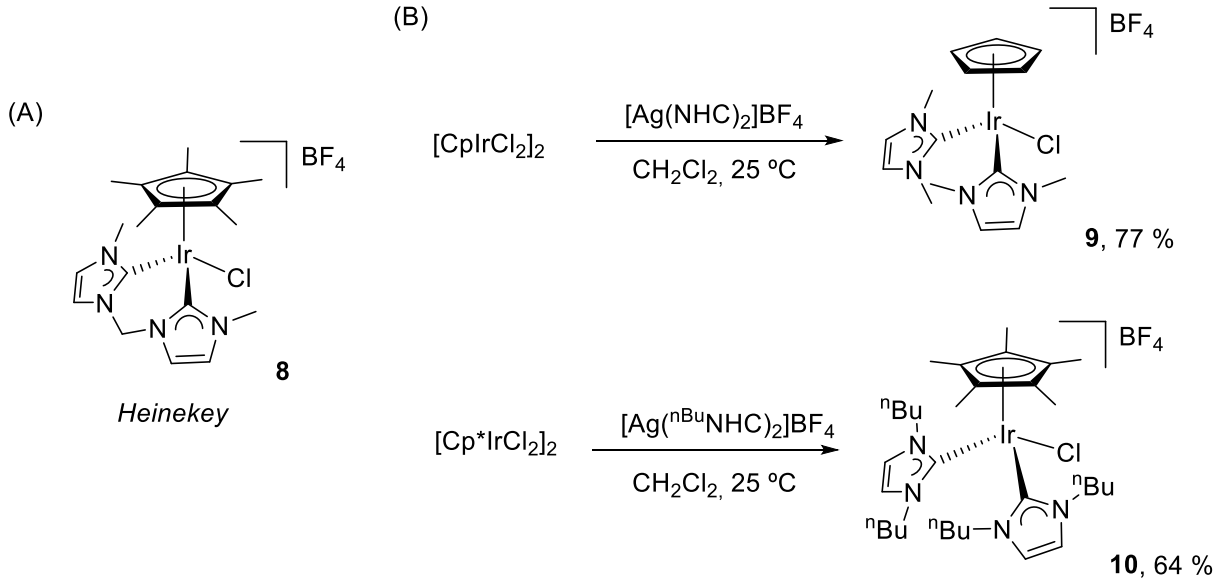

Scheme 6. Synthesis of various half-sandwich Ir-NHC complexes.

Compound **9** displays a distinct ^{1}H NMR resonance at 5.84 ppm due to the C_5H_5 ring. In contrast to complexes **3**-**5**, free rotation around the Ir-C_{NHC} bonds results in averaged signals for the

aromatic (7.07 ppm, 4 H) and aliphatic (3.48 ppm, 12 H) hydrogens of the IMe ligands, as in complexes **1** and **2**. The Cp* ligand in **10** gives rise to an intense, sharp singlet at 1.50 ppm in the ^{1}H NMR spectrum, whereas signals due to heteroaromatic (7.11 ppm) and aliphatic N-C*H*$_2$R (3.68 ppm) hydrogens of the NHC ligands appear as broad peaks at 25 ºC, likely as a result of restricted ligand rotation imposed by the greater steric bulk of the IBu ligand with respect to IMe. Variable-temperature ^{1}H NMR studies previously carried out on **1** showed decoalescence of the IMe signals at 223 K.[19] In complex **10,** the broad signal corresponding to the N-C*H*$_2$R hydrogens of the NHC ligands split into eight resonances below 243 K, with the coalescence temperature reached around 263 K (see Supporting Information, Figure S2). To quantify the energy barrier associated with the ligand rotation we carried out line-shape analysis on compounds **1** and **10** at different temperatures and analyzed the different rate constants *via* a linear free energy plot using the Eyring equation (activation parameters summarized in Table 1). As expected, the highest value of $\Delta G^{\ddagger}$ was obtained for compound **10** (16.5 ± 0.5 kcal mol^{-1}, ~7 kcal mol^{-1} higher than in **1**), reflecting high steric congestion around the metal. Interestingly, while the entropic contribution for compound **1** was almost negligible, its influence was considerable in compound **10** ($\Delta S^{\ddagger}$ = 15 ± 2 cal mol^{-1} K^{-1}), consistent with the idea that Cp* slip is required for ligand rotation in this case.

Table 1. Activation parameters obtained by ^{1}H NMR line-shape analysis and Eyring studies for the rotation of NHC ligands in Cp*Ir compounds.

Compound	**$\Delta H^{\ddagger}$ (kcal mol^{-1})**	**$\Delta S^{\ddagger}$ (cal mol^{-1} K^{-1})**	**$\Delta G_{298}^{\ddagger}$ (kcal mol^{-1})**
1	10.4 ± 0.2	2 ± 2	9.8 ± 0.5
10	21.1 ± 0.2	15 ± 2	16.5 ± 0.5

Crystals of complexes **9** and **10** suitable for X-ray diffraction were obtained by diffusion of diethyl ether into dichloromethane solution. The ORTEP diagrams of their corresponding cations are shown in Figure 8. Both Cp*Ir compounds exhibit geometries typical for these types of systems with C-Ir-C and C-Ir-Cl angles of almost 90º. The Ir-C_{NHC} bond lengths in compound **10** are slightly longer (2.050(4) and 2.084(4) Å) than in **9** (2.015(7) and 2.065(9) Å), probably due to the higher steric congestion around the iridium atom caused by the bulkier aliphatic chains.

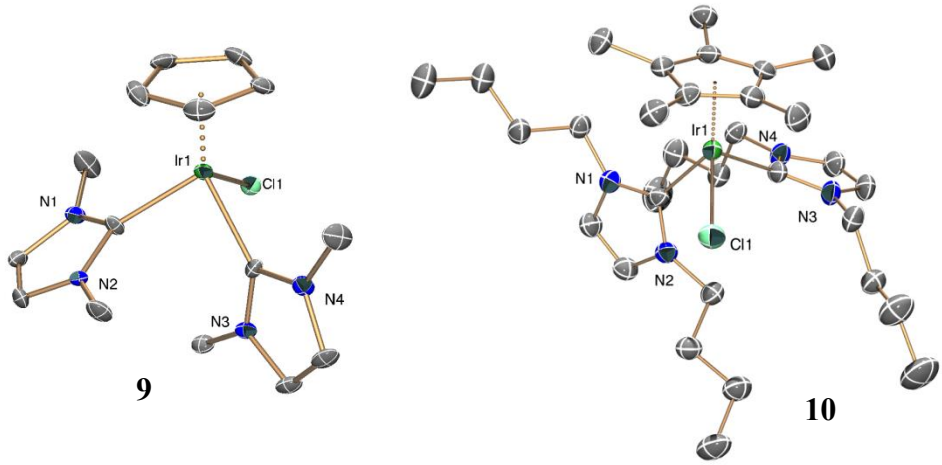

Figure 8. ORTEP diagrams of the cationic portions of compounds **9** and **10**. 50 % thermal ellipsoids are shown. Hydrogen atoms and solvent molecules have been omitted for clarity.

An interesting geometric feature of compound **10** in the solid state is a significant distortion of the Cp* ring (Figure 9). A slightly lower but noticeable distortion was also found previously in compound **1,**[19] and is the likely result of steric crowding from the NHC wingtips. In the crystal, the planes of the NHC ligands in **1** are oriented at an angle of *ca.* 70 º relative to each other, which forces one of the N-Me groups to point directly towards the Cp-Me groups, resulting in N-$CH_3\cdots H_3C$(Cp*) distances as short as 1.93 and 2.20 Å (d_{HH} in Figure 9a), compared with the sum of the conventional van der Waals radii of 2.4 Å. As a consequence, the methyl groups of the Cp* fragment are bent out of the plane of the cyclopentadienyl ring. Distortions of the methyl carbon

atoms out of the Cp* plane range from 0.17 to 0.27 Å (δ in Figure 9b). In **10** this distortion is clearly larger, with d_{HH} up to 2.35 Å and δ from 0.15 to 0.48 Å. The hindered NHC rotation in solution and Cp* distortion found in the solid state indicate significantly increased steric pressure around the iridium as compared to **1**. Although there are other examples of this kind of Cp* distortion in iridium compounds,[47] usually in the presence of bulky ligands such as *tert*-butyl phosphines, to our knowledge this is the highest distortion of this type reported for a mononuclear iridium compound. The few reported examples with slightly higher δ values include polymetallic species[48] or compounds in which the hapticity of the Cp* is considered to switch from η^5 to η^4.[49]

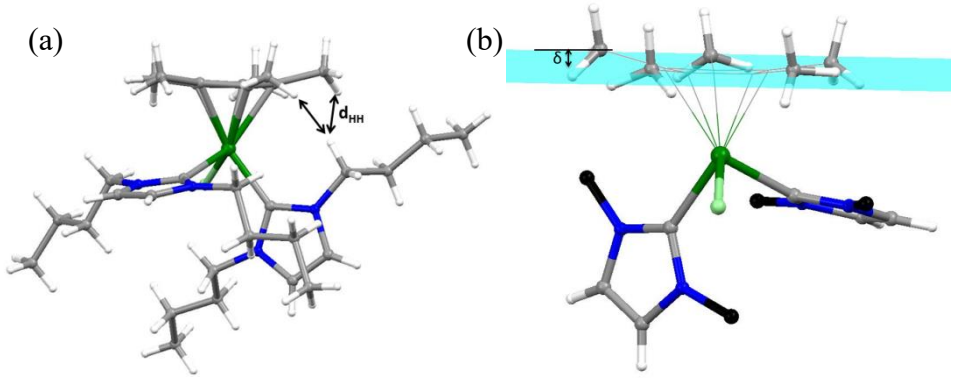

Figure 9. Solid-state structure of compound **10** emphasizing the distortion of the Cp* ring: (a) d_{HH} = shortest H-H distances between Cp* and a butyl chain; (b) δ = distance from the methyl groups of the Cp* to the cyclopentadienyl ring plane formed by the cyclopentadienyl ring (butyl chains truncated).

In contrast, in the X-ray crystal structure of complex **8**[45] the N-CH_3 termini are farther from the Cp* than in **1** or **10**, due to the different orientation brought about by the methylene linker, with the shortest d_{HH} distances being only ~2.6 Å (0.5-0.6 Å longer than in **1** and **10**). Consequently, no distortion of the Cp* ligand is observed. In compound **9** the shortest d_{HH} distance is 2.25 Å,

also indicative of some steric congestion around the iridium center, but to a much lesser extent than for **1** or **10**.

The catalytic activities of compounds **8**, **9** and **10** in transfer-hydrogenation from *iso*-propanol to acetophenone were then investigated to test whether the different degrees of steric congestion would translate into different catalytic activity. The consumption of acetophenone was monitored by *in-situ* ^{1}H NMR spectroscopy at 60ºC, and the results are summarized in Figure 6. While catalyst **1** exhibits an induction period of around 15 min under these conditions (Figure 10), increasing the steric hindrance around the metal center in compound **10** resulted in a considerable reduction of the lag phase to less than one minute, leading to complete consumption of the ketone substrate within 20 min (*ca.* 90 min using **1**). On the other hand, substitution of the C_5Me_5 ring of **1** by the less bulky C_5H_5 in **9** resulted in a remarkable enhancement of the non-productive induction period to *ca*. 90 min. This lag phase trend is perfectly consistent with higher steric pressure around Ir being favorable to the ligand loss required for precatalyst activation. If a purely ring-slippage mechanism prevailed, compound **9** would be expected to be more active than **1**,[37a] which is clearly not the case for these bis-NHC iridium complexes. In contrast, complex **8** did not display any observable induction period, although its catalytic performance was rather poor. As discussed above, the more planar geometry of the linked-bis-NHC ligand might not induce Cp* release in the way freely rotating monodentate NHCs would, and the proposed activation route based on complete Cp* loss would remain inaccessible.

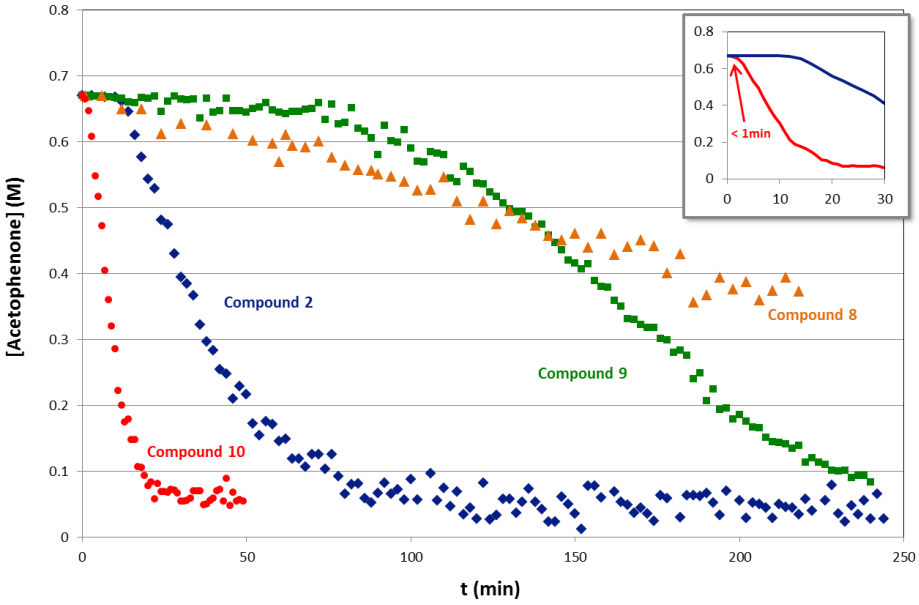

Figure 10. Profiles of acetophenone consumption monitored by ^{1}H NMR in the transfer-hydrogenation-reaction catalyzed by **2** (♦), **8** (▲), **9** (■) and **10** (●) in ^{i}PrOH (60 ºC, 1 mol % [Ir], 10 equiv. KOH, TMB as internal standard).

A plausible scenario to account for all the observed experimental data would include two distinct pathways for all half-sandwich compounds investigated in this and our prior work.[19] In compounds where the steric pressure of the spectator ligands around Ir is sufficiently high, and the lability of those ligands themselves is limited, the η^5-cyclopentadienyl moiety can be released to generate (poly)hydride complexes, at least one of which is a highly active, although less chemoselective, transfer-hydrogenation catalyst. This type of system is characterized by the presence of induction periods associated with the ring loss, high catalytic performance after the induction phase, and sensitivity to oxygen and moisture. Related to this, Papish and co-workers have recently found that the lability of arene ligands in [(η^6-C_6R_6)Ru] catalysts correlates with their activity as transfer-hydrogenation catalysts.[50] In contrast, our iridium precatalysts bearing less sterically demanding

ligands, or containing labile ligands such as pyridine, would follow one of the common monohydride mechanisms that do not require loss of the cyclopentadienyl ring. These precatalysts do not exhibit significant induction periods, and although they operate with lower rates under comparable conditions, display moderate stability toward oxygen and moisture. Complex **2** can be included into the second class of systems, since, once the monohydride is formed, Cp* loss does not seem to occur and no base is required for turnover. Starting with halide precursors such as **1, 9**, or **10** and base, however, the faster cyclopentadienyl loss pathway prevails. The observation that the induction period is second order in [Ir][19] and requires KOH appears to point to the involvement of hydroxo or alkoxo complexes as activating intermediates, but definite conclusions on this aspect cannot yet be drawn. In the future, we hope to clarify further the nature of the activation step and the active catalystspecies in these systems.

CONCLUSION

Cp*Ir compounds are extensively used as catalysts in a broad variety of transfer-hydrogenation and hydrogen-borrowing reactions. These compounds have previously been thought to operate via mechanisms in which the Cp* fragment remains bound as a robust spectator ligand. At most, reversible ring-slippage during catalysis has been postulated. Here we have found evidence that in some cases the Cp* ligand can be released under commonly employed transfer hydrogenation conditions. Model reactivity studies with phosphines have allowed us to isolate an iridium compound in which the Cp* moiety has been displaced by a diphosphine. Spectroscopic characterization and X-ray diffraction studies unequivocally demonstrated the loss of the Cp* fragment. Our new mechanistic proposal is that increasing the steric congestion in the precatalyst shortens the induction periods and thus speeds up catalysis. This effect has been demonstrated in

a series of cationic half-sandwich iridium compounds containing two NHC ligands. Remarkably, thermal pre-activation of precatalyst **1** provided a species active even at room temperature, where the parent complex **1** shows no activity under those conditions. We expect that this type of activation may also hold for some of the many known [(η^5-C_5R_5)M] catalysts, not only for transfer-hydrogenation but also other catalytic reactions where Cp loss may need to be considered as a plausible pathway

.

EXPERIMENTAL SECTION

General. Organic solvents were purified by passing over activated alumina with dry N_2. All chemicals were purchased from major commercial suppliers and used as received. *Iso*-propanol was directly purchased in 100 mL Sure/Seal^{TM} bottles and stored over molecular sieves. Syntheses were performed under an inert atmosphere of dry N_2 using standard Schlenk techniques. NMR spectra were recorded on Bruker AMX-400 and -500 spectrometers at ambient probe temperatures unless otherwise noted. Chemical shifts are reported with respect to residual internal protio solvent for ^{1}H and ^{13}C{^{1}H} NMR spectra and to an external standard for ^{31}P{^{1}H} spectra (85% H_3PO_4 in H_2O at δ 0.0 ppm). The chemical shift δ is reported in units of parts per million (ppm). MS analyses were performed by the Mass Spectrometry and Proteomics Resource of the W.M. Keck Foundation Biotechnology Resource Laboratory at Yale University. Elemental analyses were performed by Robertson Microlit Laboratories (Ledgewood, NJ, USA). Compounds (IBu)BF_4,[51] **1**,[19] **2**[19] and **8**[45] were synthesized by previously reported procedures.

[(η^5-C_5Me_5)Ir^{III}($IMe)_2$(PMe_3)](BF_4)(Cl) (3)

In the glovebox, PMe_3 (12 μL, 0.117 mmol) was added to a solution of **1** (50 mg, 0.078 mmol) in dry MeOH (5 mL), and the reaction mixture stirred for 15 min at room temperature, which resulted in a color change from dark orange to yellow. Addition of Et_2O caused the precipitation of compound **3** as a yellow microcrystalline solid (48 mg, 86 %). ^{1}H NMR (500 MHz, CD_3OD, 25 ºC): δ = 7.66 (d, 1H, $^3J_{HP}$ = 2.1 Hz, CH_{Ar}), 7.62 (d, 1H, $^3J_{HP}$ = 2.1 Hz, CH_{Ar}), 7.52 (d, 1H, $^3J_{HP}$ = 2.1 Hz, CH_{Ar}), 7.39 (d, 1H, $^3J_{HP}$ = 2.1 Hz, CH_{Ar}), 3.90 (s, 3 H, NCH_3), 3.87 (s, 3 H, NCH_3), 3.24 (s, 3 H, NCH_3), 2.75 (s, 3 H, NCH_3), 1.86 (d, 15 H, $^4J_{HP}$ = 2.3 Hz, C_5Me_5), 1.68 (d, 9 H, $^2J_{HP}$ = 10.2 Hz, $IrPMe_3$). ^{1}H NMR (500 MHz, DMSO-d_6, 25 ºC): δ = 7.76 (d, 1H, $^3J_{HP}$ = 2.0 Hz, CH_{Ar}), 7.68 (d, 1H, $^3J_{HP}$ = 2.1 Hz, CH_{Ar}), 7.67 (d, 1H, $^3J_{HP}$ = 2.1 Hz, CH_{Ar}), 7.46 (d, 1H, $^3J_{HP}$ = 2.0 Hz, CH_{Ar}), 3.78 (s, 3 H, NCH_3), 3.72 (s, 3 H, NCH_3), 3.11 (s, 3 H, NCH_3), 2.61 (s, 3 H, NCH_3), 1.74 (d, 15 H, $^4J_{HP}$ = 2.2 Hz, C_5Me_5), 1.157 (d, 9 H, $^2J_{HP}$ = 10.3 Hz, $IrPMe_3$). ^{13}C{^{1}H} NMR (125 MHz, DMSO-d_6, 25 ºC): δ = 137.3 (d, $^2J_{CP}$ = 5 Hz, Ir=C), 135.2 (d, $^2J_{CP}$ = 23 Hz, Ir=C), 127.2, 126.7, 126.7, 125.3 (CH_{Ar}), 101.2 (C_5Me_5), 41.4, 39.5, 38.9, 38.7 (NCH_3), 18.9 (d, $^1J_{CP}$ = 39 Hz, PMe_3), 10.5 (C_5Me_5). ^{31}P{^{1}H} NMR (160 MHz, CD_3OD, 25 ºC) δ: -46.9. Anal. Calcd. for $C_{23}H_{40}BClF_4IrN_4P$ (%): C, 38.47; H, 5.61; N, 7.80. Found: C, 38.87; H, 5.83; N, 7.40. HRMS (FT-ICR): calcd for $C_{23}H_{40}IrN_4P^{2+}$ (**M^{2+}**): 297.1298, 298.1305. Found: m/z = 297.1276, 298.1309. Crystal data [CCDC 973858]: $C_{24}H_{44}B_2F_8IrN_4OP$ (**3**), M = 801.42, Monoclinic, $P2_1/c$, a = 10.6139 (3) Å, b = 10.4084 (3) Å, c = 27.7107 (19) Å, β = 96.783 (7)º, V = 3039.9 (2) Å^3, Z = 4, d_{calc} = 1.751 g/cm^3, T = 150 K, 85717 reflections collected, 6913 independent reflections (R_{int} = 0.073), final R_1 = 0.0392, final wR_2 = 0.0719, GOF = 1.057.

[(η^5-C_5Me_5)Ir^{III}(IMe)$_2$(dmpm)](BF$_4$)(Cl) (4)

In the glovebox, dmpm (14 μL, 0.086 mmol) was added to a solution of **1** (50 mg, 0.078 mmol) in dry MeOH (5 mL), and the reaction mixture stirred for 15 min at room temperature, which resulted in a color change from dark orange to yellow. Addition of Et_2O caused the precipitation of compound **4** as a yellow microcrystalline solid (49 mg, 80 %). ^{1}H NMR (500 MHz, CD_3OD, 25 ºC): δ = 7.51 (d, 1H, $^3J_{HP}$ = 2.1 Hz, CH_{Ar}), 7.48 (d, 1H, $^3J_{HP}$ = 2.1 Hz, CH_{Ar}), 7.39 (d, 1H, $^3J_{HP}$ = 2.1 Hz, CH_{Ar}), 7.27 (d, 1H, $^3J_{HP}$ = 2.1 Hz, CH_{Ar}), 3.79 (s, 3 H, NCH_3), 3.75 (s, 3 H, NCH_3), 3.08 (s, 3 H, NCH_3), 2.63 (s, 3 H, NCH_3), 1.79 (br. d, 2 H, $^2J_{HP}$ = 8.6 Hz, PCH_2P), 1.71 (d, 15 H, $^4J_{HP}$ = 2.3 Hz, C_5Me_5), 1.66 (d, 3 H, $^2J_{HP}$ = 9.9 Hz, IrP*Me*Me), 1.58 (d, 3 H, ^2J = 9.9 Hz, IrPMe*Me*), 1.08 (dd, $^2J_{HP}$ = 10.6, $^4J_{HP}$ = 3.4 Hz, IrPCH_2P*Me*$_2$). ^{13}C{^{1}H} NMR (125 MHz, CD_2Cl_2, 25 ºC): δ = 139.3, 137.5 (Ir=C), 128.5, 128.2, 128.0, 126.7 (CH_{Ar}), 103.5 (C_5Me_5), 42.3, 40.7, 40.1, 39.8 (NCH_3), 35.4 (br. d, $^1J_{CP}$ = 35.3 Hz, PCH_2P), 17.0 – 16.0 (m, IrP*Me*$_2$$CH_2$P*Me*$_2$), 11.1 ($C_5$*Me*$_5$). ^{31}P{^{1}H} NMR (160 MHz, CD_2Cl_2, 25 ºC) δ: -38.7 (d, $^2J_{PP}$ = 34.9 Hz, Ir−*P*CH_2P), -53.1 (d, $^2J_{PP}$ = 34.9 Hz, Ir−PCH_2*P*). Anal. Calcd. for $C_{25}H_{45}BClF_4IrN_4P_2$ (%): C, 38.59; H, 5.83; N, 7.20. Found: C, 38.10; H, 5.72; N, 6.83. HRMS (FT-ICR): calcd for $C_{25}H_{45}IrN_4P_2^{2+}$ (**M^{2+}**): 327.1363, 328.1375. Found: m/z = 327.1350, 328.1372.

[(η^5-C_5Me_5)Ir^{III}(IMe)$_2$(dmpm=O)](BF$_4$)(Cl) (5)

A solution of **4** (30 mg, 0.046 mmol) in MeOH (3 mL) was vigorously stirred in air for 24 hours, then Et_2O was added and compound **5** precipitated as a pale yellow powder (30 mg, 97 %).^{1}H NMR (500 MHz, CD_3OD, 25 ºC): δ = 7.66 (d, 1 H, $^3J_{HP}$ = 2.1 Hz, CH_{Ar}), 7.62 (d, 1 H, $^3J_{HP}$ = 2.1 Hz, CH_{Ar}), 7.54 (d, 1 H, $^3J_{HP}$ = 2.1 Hz, CH_{Ar}), 7.41 (d, 1 H, $^3J_{HP}$ = 2.1 Hz, CH_{Ar}), 3.91 (s, 3 H, NCH_3), 3.88 (s, 3 H, NCH_3), 3.20 (s, 3 H, NCH_3), 2.77 (s, 3 H, NCH_3), 2.52 (m, 2 H, PCH_2P), 1.96 (d, 3 H, $^2J_{HP}$ = 10.0 Hz, IrP*Me*Me), 1.94 (d, 3 H, ^2J = 10.1 Hz, IrPMe*Me*), 1.85 (d, 15 H, $^4J_{HP}$

= 2.5 Hz, C_5Me_5), 1.74 (dd, $^2J_{HP}$ = 13.3, $^4J_{HP}$ = 7.4 Hz, IrPCH$_2$P(O)*Me$_2$*). ^{1}H NMR (500 MHz, DMSO-*d*$_6$, 25 ºC): δ = 7.71 (d, 1 H, $^3J_{HP}$ = 2.0 Hz, CH_{Ar}), 7.62 (d, 1 H, $^3J_{HP}$ = 2.0 Hz, CH_{Ar}), 7.61 (d, 1 H, $^3J_{HP}$ = 2.0 Hz, CH_{Ar}), 7.41 (d, 1 H, $^3J_{HP}$ = 2.1 Hz, CH_{Ar}), 3.76 (s, 3 H, NCH_3), 3.69 (s, 3 H, NCH_3), 3.05 (s, 3 H, NCH_3), 2.60 (s, 3 H, NCH_3), 2.37 (t, 2 H, $^2J_{HP}$ = 10.9 Hz, PCH$_2$P), 1.80 (d, 3 H, $^2J_{HP}$ = 10.4 Hz, IrP*Me*Me), 1.66 (d, 3 H, ^2J = 10.7 Hz, IrPMe*Me*), 1.70 (d, 15 H, $^4J_{HP}$ = 2.3 Hz, C_5Me_5), 1.55 (dd, $^2J_{HP}$ = 13.3, $^4J_{HP}$ = 6.6 Hz, IrPCH$_2$P(O)*Me$_2$*). ^{13}C{^{1}H} NMR (125 MHz, DMSO-*d*$_6$, 25 ºC): δ = 138.9, 138.4 (Ir=C), 127.2, 126.8, 126.7, 125.4, (CH_{Ar}), 101.4 (*C*$_5$Me$_5$), 40.5, 39.5, 38.9, 38.6 (NCH_3), 28.3 (PCH$_2$P), 20.0 – 17.8 (m, IrP*Me$_2$*CH$_2$P(O)*Me$_2$*), 10.2 (C_5*Me$_5$*). ^{31}P{^{1}H} NMR (160 MHz, CD_2Cl_2, 25 ºC) δ: 41.4 (d, $^2J_{PP}$ = 29 Hz, Ir−PCH$_2$*P*(O)), -39.9 (d, $^2J_{PP}$ = 29 Hz, Ir−*P*CH$_2$P). Anal. Calcd. for $C_{24}H_{45}BClF_4IrN_4OP_2$ (%): C, 37.81; H, 5.71; N, 7.06. Found: C, 38.07; H, 5.23; N, 6.70. HRMS (FT-ICR): calcd for $C_{20}H_{31}IrN_4^{2+}$ (**M^{2+}** - dmpm(O)): 259.1078, 260.1089. Found: m/z = 259.1611, 260.1612. Crystal data [CCDC 973859]: $C_{27}H_{53}B_2F_8IrN_4O_3P_2$ (**3**), M = 909.49, Orthorhombic, *P2$_1$2$_1$2$_1$*, a = 10.2065 (5) Å, *b* = 11.6450 (5) Å, *c* = 30.295 (2) Å, V = 3600.8 (4) Å^3, *Z* = 4, d_{calc} = 1.678 g/cm^3, T = 150 K, 92341 reflections collected, 6505 independent reflections (R_{int} = 0.104), final R_1 = 0.0396, final wR_2 = 0.0728, GOF = 1.088.

Reaction of 2 with two equiv. of dmpm (6, 7)

Dmpm (49 μL, 0.312 mmol) was added under argon to a solution of **1** (80 mg, 0.125 mmol) in dry MeOH (10 mL) and the mixture stirred at 70 ºC for 30 min, which resulted in a color change from orange to yellow. ^{1}H and ^{31}P{^{1}H} NMR monitoring of the reaction showed full conversion of **1** to a mixture of *ca.* 95:5 of **6** and **7**. The solution was concentrated, layered with Et$_2$O and stored at -20 ºC for crystallization. The resulting white crystals were filtered and washed with Et$_2$O to give compound **6** as colorless microcrystalline powder (70 mg, 72 %). Elemental analysis was obtained for the major compound from crystals grown from Et$_2$O/pentane. **Major compound (6).**

^{1}H NMR (500 MHz, DMSO-d_6, 25 ºC): δ 7.60 (dd, 1 H, $^{3}J_{HH}$ = 2.0, $^{5}J_{HP}$ = 0.9 Hz, CH_{Ar}), 7.51 (d, 1 H, $^{3}J_{HH}$ = 1.7 Hz, CH_{Ar}), 7.44 (dd, 1 H, $^{3}J_{HH}$ = 2.1, $^{5}J_{HP}$ = 0.9 Hz, CH_{Ar}), 7.40 (d, 1 H, $^{3}J_{HH}$ = 1.9 Hz, CH_{Ar}), 4.58 (dt, 1 H, $^{2}J_{HH}$ = 15.2, $^{2}J_{HP}$ = 10.0 Hz, $P_{(A)}CHHP_{(B)}$), 3.81 (s, 3 H, $N(CH_3)$), 3.73 (s, 3 H, $N(CH_3)$), 3.52 (dt, 1 H,$^{2}J_{HH}$ = 15.2, $^{2}J_{HP}$ = 11.5 Hz, $P_{(A)}CHHP_{(B)}$), 2.87 (s, 3 H, $N(CH_3)$), 2.86 (s, 3 H, $N(CH_3)$), 2.13 (m, 2 H, $P_{(C)}CHHP_{(D)}$), 1.93 (d, 3 H, $^{2}J_{HP}$ = 8.5 Hz, $P_{(A)}$*Me*Me), 1.90 (d, 3 H, $^{2}J_{HP}$ = 9.8 Hz, $P_{(B)}$*Me*Me), 1.85 (d, 3 H, $^{2}J_{HP}$ = 8.3 Hz, $P_{(C)}$*Me*Me), 1.67 (d, 3 H, $^{2}J_{HP}$ = 8.3 Hz, $P_{(A)}$Me*Me*), 1.45 (d, 3 H, $^{2}J_{HP}$ = 10.0 Hz, $P_{(B)}$Me*Me*), 1.30 (d, 3 H, $^{2}J_{HP}$ = 9.1 Hz, $P_{(C)}$Me*Me*), 1.21 (d, $^{2}J_{HP}$ = 3.6 Hz, 3H, $P_{(D)}$*Me*Me), 1.08 (d, 3 H, $^{2}J_{HP}$ = 3.4 Hz, $P_{(D)}$Me*Me*), -14.8 (ddt, 1 H, $^{2}J_{HP}$ = 150.0, 20.5, 5.3 Hz, Ir−H). ^{13}C{^{1}H} NMR (500 MHz, DMSO-d_6, 25 ºC): δ = 153.6 (d, $^{2}J_{CP}$ = 275 Hz, Ir=C), 151.7 (d, $^{2}J_{CP}$ = 240 Hz, Ir=C), 124.8, 124.7, 123.9, 123.5 (CH_{Ar}), 46.1 ($P_{(A)}C_2P_{(B)}$), 42.1, 41.6, 40.9, 37.3 ($N(CH_3)$), 37.2 ($P_{(C)}CH_2P_{(D)}$), 19.9 ($P_{(A)}$*Me*Me), 19.5 ($P_{(C)}$*Me*Me), 18.8 ($P_{(A)}$Me*Me*), 18.7 ($P_{(C)}$Me*Me*), 15.9 ($P_{(B)}$Me*Me*), 15.3 ($P_{(D)}$*Me*Me), 15.1 ($P_{(D)}$Me*Me*), 14.7 ($P_{(B)}$*Me*Me). ^{31}P{^{1}H} NMR (160 MHz, CD_3OD, 25 ºC): δ -43.1 (ddd, $^{2}J_{PP}$ = 63, 21, 18 Hz, Ir−$P_{(C)}$), -55.2 (ddd, $^{2}J_{PP}$ = 63, $^{4}J_{PP}$ = 21, 2 Hz, Ir−$P_{(D)}$), -76.0 (ddd, $^{2}J_{PP}$ = 26, $^{4}J_{PP}$ = 21, 2 Hz, Ir−$P_{(B)}$), -93.4 (m, Ir−$P_{(A)}$). Anal. Calcd. for $C_{20}H_{45}B_2F_8IrN_4P_4$ (%): C, 28.90; H, 5.46; N, 6.74. Found: C, 28.91; H, 5.21; N, 6.43. HRMS (FT-ICR): calcd for $C_{20}H_{45}IrN_4P_4^{2+}$ (**M^{2+}**): 328.1101, 329.1112. Found: m/z = 328.1097, 329.1002. Crystal data [CCDC 973860]: $C_{20}H_{45}B_2F_8IrN_4P_4$ (**6**), M = 831.30, Monoclinic, *P2$_1$/c*, a = 15.4119 (3) Å, *b* = 10.6410 (2) Å, *c* = 20.2231 (14) Å, β = 102.973 (7)°, V = 3231.9 (2) Å^3, *Z* = 4, d_{calc} = 1.708 g/cm^3, T = 93 K, 109528 reflections collected, 5699 independent reflections (R_{int} = 0.073), final R_1 = 0.1051, final wR_2 = 0.2288, GOF = 1.083. **Minor Compound (7)** (*ca.* 5 %) Selected NMR signals: ^{1}H NMR (500 MHz, MeOD, 25 ºC): δ 7.48, 7.32, 7.28 (CH_{Ar}), 3.92, 3.88, 3.13, 3.07 ($N(CH_3)$), -15.4 (m, Ir−H). ^{31}P{^{1}H} NMR (160 MHz, MeOD, 25 ºC): δ -54.4 (Ir−$P_{(C)}$), -73.6 (Ir−$r_{(B)}$), -92.2 (Ir−$P_{(A)}$). Crystal

data [CCDC 973861]: $C_{19}H_{44}B_2F_8IrN_4O_2P_3$ (**7**), M = 819.31, Orthorhombic, $P2_12_12_1$, a = 12.4567 (4) Å, *b* = 14.2413(5) Å, *c* = 18.0693(13) Å, V = 3205.5(3) Å^3, *Z* = 4, d_{calc} = 1.698 g/cm^3, T = 150 K, 53405 reflections collected, 5803 independent reflections (R_{int} = 0.073), final R_1 = 0.0371, final wR_2 = 0.0869, GOF = 1.013.

[(η^5-C_5H_5)Ir^{III}(IMe)(Cl)](BF$_4$) (9)

[$CpIrCl_2$]$_n$ (33 mg, 0.1 mmol) was suspended in CH_2Cl_2 (4 mL). Upon addition of dry MeCN (1 mL) a yellow solution was obtained, which was then transferred *via* cannula into a suspension of [Ag(NHC)$_2$]BF_4 (39 mg, 0.1 mmol) in CH_2Cl_2 (5 mL). The mixture was stirred under exclusion of light for 16 hours at room temperature. The colorless precipitate was filtered off and the yellow solution taken to dryness under reduced pressure. The dark yellow solid was extracted with CH_2Cl_2 (10 mL) by aid of brief sonication, filtered through a 0.2 μm PTFE filter, and concentrated to ~5 mL volume. Addition of Et_2O (15 mL) gave the product as bright yellow microcrystals, which were collected and dried in vacuo. Yield = 44 mg (77 %). ^{1}H NMR (400 MHz, CD_2Cl_2, 25 ºC): δ = 7.07 (s, 4 H, CH_{Ar}), 5.84 (s, 5 H, C_5H_5), 3.48 (s, 12 H, NCH_3). $^{13}C\{^1H\}$ NMR (100 MHz, CD_2Cl_2, 25 ºC): δ = 142.1 (Ir=C), 124.5 (CH_{Ar}), 83.8 (C_5H_5), 39.4 (NCH_3). Anal. Calcd. for $C_{15}H_{21}BClF_4IrN_4$ (%): C, 31.51; H, 3.70; N, 9.80. Found: C, 31.81; H, 3.42; N, 9.57. HRMS (FT-ICR): calcd. for $C_{15}H_{21}ClIrN_4^+$ (**M**$^+$): 483.1071, 485.1084. Found: m/z = 483.1056 and 485.1079. Crystal data [CCDC 973862]: $C_{15}H_{21}BClF_4IrN_4$ (**9**), M = 571.82, Monoclinic, $P2_1$, a = 8.4218 (4) Å, *b* = 10.3619 (4) Å, *c* = 10.7421 (8) Å, β = 102.256 (7)°, V = 916.05 (9) Å^3, *Z* = 2, d_{calc} = 2.073 g/cm^3, T = 93 K, 24830 reflections collected, 5230 independent reflections (R_{int} = 0.107), final R_1 = 0.0650, final wR_2 = 0.1069, GOF = 1.062.

[Ag(IBu)$_2$](BF$_4$)

This compound was prepared analogously as previously described.[46] $(IBu)BF_4$ (750 mg, 2.97 mmol) and Ag_2O (480 mg, 2.08 mmol) were dissolved in CH_2Cl_2 (50 mL) and a solution of NaOH (180 mg, 4.46 mmol) in deionized H_2O (15 mL) was added. The biphasic mixture was vigorously stirred overnight under exclusion of light. The aqueous phase was extracted with CH_2Cl_2 and the organics combined, washed with deionized water and filtered through a hydrophobic syringe filter (PTFE 0.2 μm). The solution was evaporated to dryness yielding $[Ag(IBu)_2](BF_4)$ as a colourless powder (610 mg, 88 %).^{1}H NMR (500 MHz, CD_2Cl_2, 25 ºC): δ = 7.05 (s, 4 H, CH_{Ar}), 4.04 (t, 8 H, $^3J_{HH}$ = 7.2 Hz, $NCH_2(\alpha)$), 1.76 (m, 8 H, $CH_2(\beta)$), 1.28 (m, 8 H, $CH_2(\gamma)$), 0.88 (t, 12 H, $^3J_{HH}$ = 7.4 Hz, $CH_3(\delta)$). $^{13}C\{^1H\}$ NMR (125 MHz, CD_2Cl_2, 25 ºC): δ = 180.2 (d, $^1J_{CAg}$ = 197 Hz, Ir=C), 122.3 (CH_{Ar}), 52.6 ($NCH_2(\alpha)$), 34.4 ($CH_2(\beta)$), 20.6 ($CH_2(\gamma)$), 14.2 ($CH_3(\delta)$). Anal. Calcd. for $C_{22}H_{40}AgN_4$ (%): C, 47.59; H, 7.26; N, 19.43. Found: C, 47.20; H, 7.43; N, 19.10. ^{1}HRMS (ESI): calcd for $C_{22}H_{40}AgN_4^+$ (**M**$^+$): 467.2304. Found: m/z = 467.2308.

[(η^5-C_5Me_5)Ir^{III}(IBu)(Cl)](BF_4) (10)

$[Cp^*IrCl_2]_2$ (100 mg, 0.126 mmol) and $[Ag(IBu)_2]BF_4$ (140 mg, 0.252 mmol) were dissolved in dry CH_2Cl_2 (10 mL), and the resulting orange suspension stirred for 24 hours at room temperature under exclusion of light. The colorless precipitate was filtered off through a pad of celite and washed with H_2O and brine. The organic phase was dried with $MgSO_4$, filtered and evaporated to dryness to give compound **10** as an orange waxy solid (130 mg, 64 %). ^{1}H NMR (500 MHz, CD_2Cl_2, 25 ºC): δ = 7.11 (s, 4 H, CH_{Ar}), 3.68 (br. s, 8 H, $NCH_2(\alpha)$), 1.63 – 1.45 (m, 8 H, $CH_2(\beta)$), 1.50 (s, 15 H, C_5Me_5), 1.25 (m, 8 H, $CH_2(\gamma)$), 0.87 (t, 12 H, $^3J_{HH}$ = 7.4 Hz, $CH_3(\delta)$). ^{1}H NMR (400 MHz, CD_2Cl_2, -60 ºC): δ = 7.29 (br. s, 1 H, CH_{Ar}), 7.16 (br. s, 2 H, CH_{Ar}), 7.08 (br. s, 1 H, CH_{Ar}), 4.63 (dt, 1 H, $^3J_{HH}$ = 12.5, $^2J_{HH}$ = 4.9 Hz, $NCH_2(\alpha)$), 4.08 (br. t, 1 H, $^3J_{HH}$ = 8.5 Hz, $NCH_2(\alpha)$), 3.89 (dt, 1 H, $^3J_{HH}$ = 12.1, $^2J_{HH}$ = 4.6 Hz, $NCH_2(\alpha)$), 3.76 (m, 1 H, $NCH_2(\alpha)$), 3.89 (m, 1 H, $NCH_2(\alpha)$),

3.44 (dt, 1 H, $^{3}J_{HH}$ = 12.5, $^{2}J_{HH}$ = 5.5 Hz, $NCH_2(\alpha)$), 2.97 (dt, 1 H, $^{3}J_{HH}$ = 12.2, $^{2}J_{HH}$ = 4.9 Hz, $NCH_2(\alpha)$), 2.75 (br. t, 1 H, $^{3}J_{HH}$ = 12.8, $NCH_2(\alpha)$), 1.84, 1.50 (br. m, 4 H each, $CH_2(\beta)$), 1.55 (s, 15 H, C_5Me_5), 1.48, 1.18 (br. m, 4 H each, $CH_2(\gamma)$), 1.06 – 0.71 (m, 12 H, $CH_3(\delta)$). $^{13}C\{^{1}H\}$ NMR (125 MHz, CD_2Cl_2, 25 ºC): δ = 147.1 (Ir=C), 122.6 (br. s, CH_{Ar}), 96.6 (C_5Me_5), 51.1 (br. s, $NCH_2(\alpha)$), 33.3 ($CH_2(\beta)$), 20.8 ($CH_2(\gamma)$), 14.4 ($CH_3(\delta)$), 10.8 (C_5Me_5). Anal. Calcd. for $C_{32}H_{55}BClF_4IrN_4$ (%): C, 47.43; H, 6.84; N, 6.91. Found: C, 47.28; H, 6.59; N, 6.65.HRMS (FT-ICR): calcd for $C_{32}H_{56}IrN_4^+$ (**MH**$^+$ – Cl): 687.4111, 689.4134. Found: m/z = 687.4112, 689.4107. Crystal data [CCDC 973863]: $C_{36}H_{63}BClF_4IrN_4O$ (**10**), M = 882.36, Monoclinic, $P2_1/c$, a = 13.9451 (10) Å, b = 22.7483 (4) Å, c = 13.5566 (3) Å, β = 112.440 (8)°, V = 3974.9 (3) Å^3, Z = 4, d_{calc} = 1.474 g/cm^3, T = 150 K, 219215 reflections collected, 9120 independent reflections (R_{int} = 0.109), final R_1 = 0.0471, final wR_2 = 0.0827, GOF = 1.078.

Catalysis. Catalytic runs were performed by charging a flame-dried Schlenk flask with 20 µmol Ir-complex and 0.2 mmol 1,3,5-trimethoxybenzene (TMB) as internal standard under N_2 and adding 2 mL dry *iso*-propanol. After heating to the desired reaction temperature liquid substrate (2 mmol acetophenone) and base (0.2 mmol KOH, semiconductor grade) were added in 1 mL dry iso-propanol to start the reaction. Aliquots were withdrawn by syringe and quenched by mixing with $CDCl_3$ in air at room temperature. After filtration through celite the solution was analyzed for conversion by ^{1}H-NMR. *In-situ* NMR reaction progress monitoring was performed in screw-capped 5 mm NMR tubes, charged with solid Ir-complex (0.007 mmol) and 1,3,5-trimethoxybenzene (0.067 mmol) under N_2. A solution of KOH (0.067 mmol) in dry iso-propanol (1 mL) was added, followed by acetophenone (78 µL, 0.67 mmol). The NMR tube was sonicated for 30 seconds, placed in the NMR spectrometer with the probe preheated to 60 ºC, and ^{1}H NMR spectra acquired every 2 minutes.

Hammett studies. The procedure described above for *in-situ* NMR reaction progress was followed under competitive and non-competitive conditions. In the former case ~~In these studies~~, 1 mmol of acetophenone and 1 mmol of *para*-substituted acetophenone were added following addition of *iso*-propanol. First-order kinetic plots for ketone consumption allowed obtaining k_H and k_X as the first-order kinetic rate constants for acetophenone and *para*-substituted acetophenone, as well as corresponding standard deviations σ_H and σ_X derived from regression analysis. The Hammett plot of Figure 5 was constructed using those data and tabulated substituent constants (σ).[52] The error bars were estimated as three standard deviations (99.7 % confidence) after applying error propagation calculations and assuming an error of ±0.5 K for the temperature of the NMR probe.

Kinetic isotopic effect studies. The procedure described above for *in-situ* NMR reaction progress was followed for competitive and non-competitive KIE experiments using **1** and **2**. In the former case, the reduction of the *p*-chloro acetophenone (used instead of acetophenone for more accurate integration) was followed by adding 0.5 mL of deuterated *iso*-propanol-(d_8) and 0.5 mL of non-deuterated *iso*-propanol. Primary kinetic isotopic effects were determined as the ratio between non-deuterated and deuterated products, which was approximately constant over the reaction progress. Non-competitive KIEs ($KIE = k_H/k_D$) were determined as the ratio between first-order kinetic rate constants obtained by the common procedure for *in-situ* NMR experiments carried out in *iso*-propanol (k_H) and labeled *iso*-propanol(d_8) (k_D).

ASSOCIATED CONTENT

Supporting Information. Details of crystallographic analyses, CIF files, original NMR spectra of new compounds, variable-temperature NMR spectra of compound **10** and Eyring analysis for solution dynamic ^{1}H NMR of **1** and **10**, FT-ICR analysis of *post*-catalytic transfer-hydrogenation reaction. This material is available free of charge via the Internet at http://pubs.acs.org.

AUTHOR INFORMATION

Corresponding Authors

*E-mail: u.hintermair@bath.ac.uk (U. H.).

*E-mail: robert.crabtree@yale.edu (R. H. C.).

Author Contributions

The manuscript was written through contributions of all authors. All authors have given approval to the final version of the manuscript.

Notes

The authors declare no competing interest.

ACKNOWLEDGMENT

This material is based in part upon work supported by the Center for Catalytic Hydrocarbon Functionalization, an Energy Frontier Research Center funded by the U.S. Department of Energy, Office of Science, Office of Basic Energy Sciences, under Award Number DE-SC0001298 (R. H. C., U. H. and J. C., synthesis.), by the U.S. Department of Energy, Office of Science, Office of Basic Energy Sciences catalysis award (J.C., DE-FG02-84ER13297, catalysis), and U.S. DoE Award 1043588 (T.P.B., characterization.). U.H. also thanks the Alexander von Humboldt

Foundation for a Feodor Lynen Research Fellowship, supplemented by a grant from the Yale Institute for Nanoscience and Quantum Engineering, and the Centre for Sustainable Chemical Technologies at the University of Bath for a Whorrod Research Fellowship. We thank Nathan Schley (Caltech) and Mike Whittlesey (Bath) for valuable discussions.

GRAPHICAL ABSTRACT

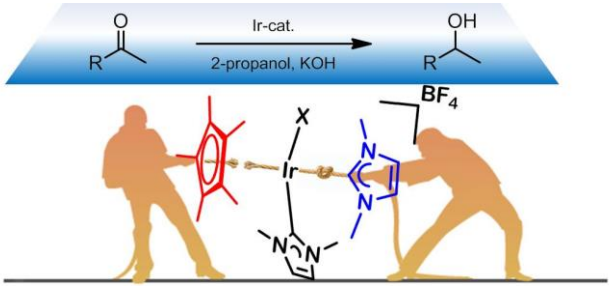

REFERENCES

[1] Klomp, D.; Hanefeld, U.; Peters, J. A. In *The Handbook of Homogeneous Hydrogenation*; Vries, J. G. d., Elsevier, C. J., Eds.; Wiley-VCH: Weinheim, **2007**; Vol. 3, p 585-630.

[2] Bullock, R. M. *Chem. Eur. J.* **2004**, *10*, 2366-2374.

[3] Guillena, G.; Ramón, D. J.; Yus, M. *Ang. Chem. Int. Ed.* **2007**, *46*, 2358-2364.

[4] Nixon, T. D.; Whittlesey, M. K.; Williams, J. M. J. *Dalton Trans.* **2009**, 753-762.

[5] Dobereiner, G. E.; Crabtree, R. H. *Chem. Rev.* **2009**, *110*, 681-703.

[6] Watson, A. J. A.; Williams, J. M. J. *Science* **2010**, *329*, 635-636.

[7] Guerbet, M. C. R. *Acad. Sci.* **1909**, *49*, 129-132.

[8] Haddad, Y. M. Y.; Henbest, H. B.; Husbands, J.; Mitchell, T. R. B. *Proc. Chem. Soc.* **1964**, 361.

[9] Trocha-Grimshaw, J.; Henbest, H. B. *Chem. Commun.* **1967**, 544-544.

[10] Henbest, H. B.; Mitchell, T. R. B. *J. Chem. Soc. C: Organic* **1970**, 785-791.

[11] Suzuki, T. *Chem. Rev.* **2011**, *111*, 1825-1845.

[12] Murata, K.; Ikariya, T.; Noyori, R. *J. Org. Chem.* **1999**, *64*, 2186-2187.

[13] Ikariya, T.; Blacker, A. J. *Acc. Chem. Res.* **2007**, *40*, 1300-1308.

[14] Fujita, K.-i.; Yamaguchi, R. *Synlett* **2005**, *4*, 560-571.

[15] Saidi, O.; Williams, J. M. J. *Top. Organomet. Chem.* **2011**, *34*, 77-106.

[16] (a) Hanasaka, F.; Fujita, K.-i.; Yamaguchi, R. *Organometallics* **2005**, *24*, 3422-3433. (b) Corberán, R.; Peris, E. *Organometallics* **2008**, *27*, 1954-1958. (c) Azua, A.; Mata, J. A.; Peris, E.; Lamaty, F.; Martinez, J.; Colacino, E. *Organometallics* **2012**, *31*, 3911-3919.

[17] (a) Bartoszewicz, A.; Marcos, R.; Sahoo, S.; Inge, A. K.; Zou, X.; Martín-Matute, B. *Chem. Eur. J.* **2012**, *18*, 14510-14519. (b) Blanco, M.; Álvarez, P.; Blanco, C.; Jiménez, M. V.; Fernández-Tornos, J.; Pérez-Torrente, J. P.; Oro, L. A.; Menéndez, R. *ACS Catal* **2013**, *3*, 1307-1317. (c) Zuo, W.; Braunstein, P. *Organometallics* **2012**, *31*, 2606-2615.

[18] Berliner, M. A.; Dubant, S. p. P. A.; Makowski, T.; Ng, K.; Sitter, B.; Wager, C.; Zhang, Y. *Org. Proc. Res. Dev.* **2011**, *15*, 1052-15062.

[19] Hintermair, U.; Campos, J.; Brewster, T. P.; Pratt, L. M.; Schley, N. D.; Crabtree, R. H. *ACS Catal.* **2014**, *4*, 99-108.

[20] Samec, J. S. M.; Bäckvall, J.-E.; Andersson, P. G.; Brandt, P. *Chem. Soc. Rev.* **2006**, *35*, 237-248.

[21] (a) Verley, A. *Bull. Soc. Chim. Fr.* **1925**, *37*, 537. (b) Meerwin, H.; Schmidt, R. *Liebigs Ann.* **1925**, *444*, 221-238.

[22] Handgraaf J-W.; Reek J. N. H.; Meijer E. J. *Organometallics*, **2003**, *22*, 3150-3157.

[23] (a) Hashigushi, S.; Fujii, A.; Takehera, J.; Ikariya, T.; Noyori, R. *J. Am. Chem. Soc.* **1995**, *117*, 7562-7563. (b) Yamakawa, M.; Ito, H.; Noyori, R. *J. Am. Chem. Soc.* **2000**, *122*, 1466-1478. (c) Haack, K. J.; Hashiguchi, S.; Fujii, A.; Ikariya, T.; Noyori, R. *Angew. Chem. Int. Ed.* **1997**, *36*, 285-288.

[24] Zassinovich, G.; Mestroni, G.; Gladiali, S. *Chem. Rev.* **1992**, *92*, 1051-1069.

[25] (a) Fujita, K. I.; Yoshida, T.; Imori, I.; Yamaguchi, R. *Org. Lett.*, **2011**, *13*, 2278-2281. (b) Li, H.; Lu, G.; Jiang, J.; Huang, F.; Wang, Z.-X. *Organometallics*, **2011**, *30*, 2349-2363; (c) Azerraf, C.; Gelman, D. *Chem.–Eur. J.* **2008**, *14*, 10364-10368.

[26] Pàmies, O.; Bäckvall, J.-E. *Chem. Eur. J.* **2001**, *7*, 5052-5058.

[27] Although BHE at coordinatively saturated TM complexes usually requires temporary ligand dissociation to free up an adjacent vacant site (Blum, O.; Milstein, D. *J. Am. Chem. Soc*. **1995**, *117*, 4582-4594), bimolecular pathways (Ritter, J. C. M.; Bergman, R. G. *J. Am. Chem. Soc.* **1998**, *120*, 6826-6827) and solvent-assisted dissociative pathways (Smythe, N. A.; Grice, K. A.;

Williams, B. S.; Goldberg, K. I. *Organometallics*, **2009**, *28*, 277-288) have also been suggested that would proceed without a second open site on the metal.

[28] O, W. W. N.; Lough, A. J.; Morris, R. H. *Organometallics* **2012**, *31*, 2152-2165.

[29] (a) Ogo, S.; Abura, T.; Watanabe, Y. *Organometallics* **2002**, *21*, 2964-2969. (b) Ghebreyessus, K. Y.; Nelson, J. H. *J. Organomet. Chem* **2003**, *669*, 48-56.

[30] Smith, K. T.; Roemming, C.; Tilset, M. *J. Am. Chem. Soc.* **1993**, 115, 8681-8689.

[31] Hounjet, L. J.; Ferguson, M. J.; Cowie, M. *Organometallics*, **2011**, *30*, 4108-4114..

[32] Aranyos, A.; Csjernyik, G.; Szabó, K. J.; Bäckvall, J.-E. *Chem. Commun.* **1999**, 351-352.

[33] Hansch, C.; Leo, A.; Taft, R. W. *Chem. Rev.* **1991**, *91*, 165-195.

[34] Crudden, C. M.; Allen, D. P. *Coord. Chem. Rev.* **2004***, 248*, 2247-2273.

[35] (a) Trnka, T. M.; Morgan, J. P.; Sanford, M. S.; Wilhelm, T. E.; Scholl, M.; Choi, T.; Ding, S.; Day, M. W.; Grubbs, R. H. *J. Am. Chem. Soc.* **2003**, *125*, 2546-2558. (b) Allen, D. P.; Crudden, C. M.; Calhoun, L. A.; Wang, R. *J. Organomet. Chem.* **2004**, *689,* 3203-3209. (c) McGuinness, D. S.; Green, M. J.; Cavell, K. J.; Skelton, B. W.; White, A. H. *J. Organomet. Chem.* **1998**, *565*, 165-178. (d) McGuinness, D. S.; Cavell, K. J. *Organometallics* **2000**, *19,* 4918-4920. (e) Martin, H. C.; James, N. H.; Aitken, J.; Gaunt, J. A.; Adams, H.; Haynes, A. *Organometallics* **2003**, *22*, 4451-4458.

[36] (a) Hintermair, U.; Sheehan, S. W.; Parent, A. R.; Ess, D. H.; Richens, D. T.; Vaccaro, P. H.; Brudvig, G. W.; Crabtree, R. H. *J. Am. Chem. Soc.* **2013**, *135*, 10837-10851. (b) Wang, C.; Wang, J.-L.; Lin, W. *J. Am. Chem. Soc.* **2012**, *134*, 19895-19908. (c) Grotjahn, D. B.; Brown, D. B.;

Martin, J. K.; Marelius, D. C.; Abadjian, M.-C.; Tran, H. N.; Kalyuzhny, G.; Vecchio, K. S.; Specht, Z. G.; Cortes-Llamas, S. A.; Miranda-Soto, V.; van Niekerk, C.; Moore, C. E.; Rheingold, A. L. *J. Am. Chem. Soc.* **2011**, *133*, 19024-19027. (d) Park-Gehrke, L. S.; Freudenthal, J.; Kaminsky, W.; DiPasquale, A. G.; Mayer, J. M. *Dalton Trans.* **2009**, 1972-1983. (e) Savini, A.; Belanzoni, P.; Bellachioma, G.; Zuccaccia, C.; Zuccaccia, D.; Macchioni, A. *Green Chem.* **2011**, *13*, 3360-3374. (f) Zuccaccia, F.; Bellachioma, G.; Bolaño, S.; Rocchigiani, L.; Savini, A.; Macchioni, A. *Eur. J. Inorg. Chem.* **2012**, 1462-1468.

[37] (a) O'Connor, J. M.; Casey, C. P. *Chem. Rev.* **1987**, *87*, 307-318. (b) Veiros, L. F. *Organometallics*, **2000**, *19*, 5549-5558. (c) Liu, R.; Zhou, X. *J. Organomet. Chem.* **2007**, *692*, 4424-4435.

[38] (a) Jutzi, P.; Reumann, G. *J. Chem. Soc., Dalton Trans.* **2000**, 2237-2482. (b) Shapiro, P. J.; Vij, A.; Yap, G. P. ; Rheingold, A. L. *Polyhedron* **1995**, *14*, 203-209. (c) Carmona, E.; del Mar Conejo, M.; Fernández, R.; Andersen, R. A.; Gutiérrez-Puebla, E.; Monge, M. A. *Chem. Eur. J.* **2003**, *9,* 4462-4471. (d) Jutzi, P.; Meyer, U.; Opiela, S.; Neumann, B.; Stammler, H. G. *J. Organomet. Chem.* **1992**, *439*, 279-301. (e) Holtmann, U.; Jutzi, P.; Kühler, T.; Neumann, B.; Stammler, H. G. *Organometallics* **1999**, *18*, 5531-5538.

[39] Hanusa, T. P. *Organometallics*, **2002**, *21*, 2559-2571.

[40] See for example: (a) Leontyeva, L.; Hughes, R. P.; Rheingold, A. L. *Organometallics*, **2007**, *26*, 5735-5736. (b) Tetrick, S. M.; Cutler, A. R. *Organometallics* **1999**, *18*, 1741-1746. (c) Simanko, W.; Sapunov, V. N.; Schmid, R.; Kirchner, K.; Wherland, S. *Organometallics* **1998**, *17*, 2391-2393. (d) Casey, C. P.; O'Connor, J. M. *J. Am. Chem. Soc.* **1983**, *105*, 2919-2920. (e) Prinza,

M.; Veiros, L. F.; Calhorda, M. J.; Romao, C. C.; Herdtweck, E.; Kuhn, F. E.; Herrmann, W. A. *J. Organomet. Chem.* **2006**, *691*, 4446-4458.

[41] Casey, C. P.; O'Connor, J. M.; Haller, K. J. *J. Am. Chem. Soc.* **1985**, *107*, 1241-1246.

[42] (a) Aballay, A.; Arancibia, R.; Buono-Core, G. E.; Cautivo, T.; Godoy, F.; Klahn, A. H.; Oelckers, B. *J. Organomet. Chem.* **2006**, *691*, 2563-2566. (b) Hughes, R. P.; Lindner, D. C.; Rheingold, A. L.; Yap, G. P. A. *Organometallics* **1996**, *15*, 5678-5686. (c) Klahn, A. H.; Arenas, S. *Bol. Soc. Chil. Quim.* **1993**, *38*, 277-283. (d) Pedersen, A.; Tilset, M. *Organometallics*, **1993**, *12*, 3064. (e) Oldham, W. J. Jr.; Hinkle, A. S.; Heinekey, D. M. *J. Am. Chem. Soc.* **1997**, *119*, 11028.

[43] (a) Evans, W. J.; Perotti, J. M.; Kozimor, S. A.; Champagne, T. M.; Davis, B. L.; Nyce, G. W.; Fujimoto, C. H.; Clark, R. D.; Johnston, M. A.; Ziller, J. W. *Organometallics* **2005,** *24,* 3916-3931. (b) Evans, W. J.; Forrestal, K. J.; Ziller, J. W. *J. Am. Chem. Soc.* **1995**, *117,* 12635-12636. (c) Schumann, H.; Glanz, M.; Hemling, H.; Gerlitz, F. H. *J. Organomet. Chem.* **1993**, *462*, 155-161. (d) Demir, S.; Mueller, T. J.; Ziller, J. W.; Evans, W. J. *Angew. Chem. Int. Ed.* **2011**, *50*, 515-518.

[44] An alternative pathway involving nucleophilic attack of dmpm on the Cp* (Chin, C. S.; Kim, Y.; Lee, H. *Inorg. Chim. Acta.* **2004**, *357*, 3064-3070) would not apply in this case, since 2 equiv of phosphine lead to quantitative formation of compounds **6** and **7**.

[45] Vogt, M.; Pons, V.; Heinekey, D. M. *Organometallics* **2005**, *24*, 1832-1836.

[46] Hintermair, U.; Englert, U.; Leitner, W. *Organometallics* **2011**, *30*, 3726-3731.

[47] (a) Grotjahn, D. B.; Kraus, J. E.; Amouri, H.; Rager, M. –N.; Cooksy, A. L.; Arita, A. J.; Cortes-Llamas, S. A.; Mallari, A. A.; DiPasquale, A. G.; Moore, C. E.; Liable-Sands, L. M.; Golen, J. D.; Zakharov, L. N.; Rheingold, A. L. *J. Am. Chem. Soc.* **2010**, *132*, 7919-7934. (b) Hughes, R. P.; Lindner, D. C.; Smith, J. M.; Zhang, D.; Incarvito, C. D.; Lam, K. –C.; Liable-Sands, L. M.; Sommer, R. D.; Rheingold, A. L. *Dalton Trans.* **2001**, 2270-2278. (c) Hughes, R. P.; Smith, J. M.; Incarvito, C. D.; Lam, K. –C.; Rhatigan, B.; Rheingold, A. L. *Organometallics*, **2002**, *21*, 2136-2144.

[48] (a) Kochi, T.; Nomura, Y.; Tang, Z.; Ishii, Y.; Mizobe, Y.; Hidai, M. *Dalton Trans.* **1999**, 2575. (b) Srinivasan, P.; Leong, W. K. *J. Organomet. Chem.* **2006**, *691*, 403-412.

[49] Tanaka, K.; Kushi, Y.; Tsuge, K.; Toyohara, K.; Nishioka, T.; Isobe, K. *Inorg. Chem.* **1998**, *37*, 120-126.

[50] DePasquale, J.; Kumar, M.; Zeller, M.; Papish, R. T. *Organometallics* **2013**, *32*, 966-979.

[51] (a) Sanjay S. Palimkar, Shapi A. Siddiqui, Thomas Daniel, Rajgopal. J. Lahoti, Kumar V. Srinivasan *J. Org. Chem.* **2003**, *68*, 9371-9378. (b) Dinarés, I.; Garcia de Miguel, C.; Ibáñez, A.; Mesquida, N.; Alcalde, E. *Greem Chem.* **2009**, *11*, 1507-1510.

[52] Hansch, C.; Leo, A.; Taft, R. W. *Chem. Rev.* **1991**, *91*, 165-195.